Groundwater Recharge Estimation in Thepkasattri Watershed Phuket, Thailand

Yacob Tesfamariam Tesfaldet

A Thesis Submitted in Fulfillment of the Requirement for Degree of

Master of Science in Earth System Science

Prince of Songkla University

2019

Groundwater Recharge Estimation in Thepkasattri Watershed Phuket, Thailand

Yacob Tesfamariam Tesfaldet

A Thesis Submitted in Fulfillment of the Requirement for Degree of

Master of Science in Earth System Science

Prince of Songkla University

2019

Thesis Title	Groundwater Recharge Estimation in Thepkasattri Watershed Phuket, Thailand
Author	Mr. Yacob Tesfamariam Tesfaldet
Major Program	Earth System Science

Major Advisor

……
(Dr. Avirut Putiwongrak)

Examining Committee:

……Chairperson
(Assoc. Prof. Dr. Pham Huy Giao)

….……Committee
(Asst. Prof. Thongchai Suteerasak)

….……Committee
(Dr. Tanwa Arpornthip)

….……Committee
(Dr. Avirut Putiwongrak)

The Graduate School, Prince of Songkla University, has approved this thesis as fulfillment of the requirements for the Master of Science Degree in Earth System Science

……
(Prof. Dr. Damrongsak Faroongsarng)
Dean of Graduate School

This is to certify that the work here submitted is the result of the candidate's own investigations. Due acknowledgement has been made of any assistance received.

.....Signature

(Dr. Avirut Putiwongrak)

Major Advisor

.....Signature

(Mr. Yacob Tesfamariam Tesfaldet)

Candidate

I hereby certify that this work has not been accepted in substance for any degree, and is not being currently submitted in candidature for any degree.

.....Signature

(Mr. Yacob Tesfamariam Tesfaldet)

Candidate

Thesis Title Groundwater Recharge Estimation in Thepkasattri Watershed Phuket, Thailand

Author Mr. Yacob Tesfamariam Tesfaldet

Major Program Earth System Science

Academic Year 2018

ABSTRACT

Groundwater recharge is an important issue for places like Phuket Island, where the fresh water supply is heavily depending on groundwater. Therefore, considering the growing demand y for freshwater and rapidly increasing the population. It is important to investigate the spatial and temporal variation in recharge. In this study groundwater recharge estimation and seasonal groundwater, recharge characterization has been done in Thepkasattri sub-district. Groundwater recharge estimation was done using the chloride mass balance (CMB) and the water table fluctuation method (WTF) method. While seasonal groundwater recharge characterization was done using time-lapse ERT in two locations. The objective of this study is to quantify annual recharge in Thepkasattri and to investigate the seasonal infiltration characteristic through the vadose zone. Based on the CMB method recharge in Thepkasattri varies between 443 to 1439 mm/yr. with mean recharge of 1172 mm/yr. The mean recharge accounts for 47% of the annual rainfall in Thepkasattri.

On the other hand, recharge estimated using the WTF method varies from 349 to 552 mm/yr. The average is 418 mm/yr. and this represents 19% of annual precipitation. The recharge estimated using the WTF method falls in the range of 443 to 1439 mm/yr. estimated using the CMB method. There is some uncertainty associated with the WTF method due to lack of water table data that represent the calendar year. Evapotranspiration was estimated using concentration factor (CF) and found to be 53% of annual rainfall. Moreover, spatial variability of recharge is strongly related to the hydraulic property of the unsaturated zone and the land cover of the area.

Seasonal groundwater recharge characterization using time-lapse ERT was done in two lines at three dates (March, June, and September in 2018). The location of ERT lines was one on vadose zone composed of alluvial deposit and the second is in weathered granite; the lines were oriented at an angle to the nearby passing stream drainage. Time-lapse ERT in line one shows -100% change in resistivity from dry season to wet season. This change was attributed due to water infiltration through the unsaturated zone and the stream. While in line two -75% of resistive decrease was observed. The change in resistivity was attributed to surficial infiltration through the vadose zone. Based on the relationship established by earlier researchers the decrease in resistivity indicates the degree of water saturation. Therefore, change in resistivity in both locations further indicates the degree of water saturation in the vadose zone. The study further suggests recharge in the study area is episodic that has a direct effect of climatic condition.

Keywords: Groundwater, Recharge, CMB, WTF, time-lapse ERT, IDW, Resistivity, Thepkasattri.

ACKNOWLEDGMENT

First I would like to give thanks to God almighty for the strength and good health to carried out my study. This thesis is a result of encouragement and assistance from my teachers, family and friends, and I greatly acknowledge their contribution. Particularly, I greatly appreciate Dr. Avirut Puttiwongrak, Dr. Tanwa Arpornthip, and Bereket T. Tesfaldet. I am indebted to Ratha Men, Vann Sakannan, Naung Naung Htwe, Mai Khanh Phoung, Julius Mmavele, and Malte Henning for the generous advice, assistance, and valuable comments. At last but not least I greatly appreciate the great assistance of Eduardo Rodrigues and Jason Greenwood from AGI technical support team.

Yacob T. Tesfaldet

CONTENTS

CONTENTS (Continued)

CONTENTS (Continued)

LIST OF FIGURES

LIST OF FIGURES (Continued)

LIST OF TABLES

LIST OF ABBREVIATIONS

Cl^- or Cl – Chloride

CF – Concentration Factor

CMB – Chloride Mass Balance

CV – Coefficient of Variation

DD – Dipole-dipole

DEM – Digital Elevation Model

DGR – Department of Groundwater Resources

EC – Electrical conductivity

ERT – Electrical Resistivity Tomography

ET_f – Evapotranspiration

GW – Groundwater

IDW – Inverse Distance Weight

IEC – International Electrotechnical Commission

ISO – International Organization for Standardization

L2 – Least squares

MBGL – Meters Below Ground Level

mg/l – Milligram per Liter

mm/yr. – Millimeter per year

S-W – Shapiro-Wilk

SWB – Soil Water Balance

VES – Vertical Electrical Sounding

WTF – Water Table Fluctuation

CHAPTER 1

INTRODUCTION

1.1 Background of the study

Water has a vital role in our daily life including our well-being in terms of health and sanitation. This is evident by the amount of water consumed all over the world. Even though 71% of our planet is covered by water bodies, fresh water constitutes only 3.5% of all water (Williams, 2017). The main sources of fresh water are groundwater, glacial, lakes and streams; groundwater accounts for 30% of all freshwater bodies (Covitt et al., 2012). This makes groundwater a valuable resource for fresh water supply. However, groundwater faces two key challenges; these are overexploitation and contamination. Groundwater protection from depletion and pollution is the prime challenges our planet faces today. Therefore, to protect groundwater from degradation, the hydrogeological parameters of the aquifers should be well defined. The most important parameters are the hydraulic conductivity, Storativity, recharge, and transmissivity.

Since the birth of the field hydrogeology, different methods are developed to measure the hydrogeological parameters of an aquifer. However, a single method approach is not applicable and reliable to define the complex hydrogeological phenomena. Therefore, researchers are using an integrated approach of different methods to enhance the information. Groundwater recharge varies in space and time, which in turn depends on the amount of infiltration and the geology of vadose zone. The vertical electrical sounding (VES) method can give information on the resistivity of the vadose zone. While recharge estimation can be done using environmental tracer, chemical tracers, water balance, water table fluctuation approach and so on. However, the reliability of estimation depends on the integration of methods. Although integrated approach might not reduce uncertainty, it validates the conceptual model of consistency of different methods (Healy, 2012).

1.2 Statement of the Problem

Phuket is the largest island in Thailand with an area of 576 square kilometers and around 537 thousand populations. The island is one of the world's most attractive tourist destinations. As a result, the number of tourists visiting the island is increasing annually. For example, the number of tourists visited Phuket in the year 2009 was 2.5 million and this number increased in the year 2013 to 9.0 million (M-BRACE, 2014). Associated with the increasing population and the warm temperature of the island, fresh water consumption is very high and is showing a dramatic increase due to the mentioned factors. For example, at present, the water demand is increasing exponentially with an annual increment of 10 to 20% (Kong, 2017). Because Phuket is an Island situated in Andaman sea, there is no water supply form the mainland. Therefore, the major source of fresh water in Phuket is groundwater, which makes 68.14% of the water supply (Kong, 2017). Most of the potential groundwater aquifers are found in alluvial sediments, weathered and fractured granitic rocks. Sustainable usage of groundwater resource depends on the appropriate quantification of output (discharge) and input (recharge). Therefore, the estimation of groundwater recharge is a key factor in groundwater resource management and protection.

However, very few studies have been done to estimate the annual recharge of groundwater in Phuket. Hence water uptake in relation to intake is not known and as a consequence groundwater resource in Phuket is vulnerable to mismanagement and pollution. Consequently, groundwater recharge estimation is becoming increasingly pertinent in Phuket where most of the water demand depends on groundwater. Besides, the concerned body can decide on water resource management and budgeting. In response to this problem, this study proposes a detailed investigation of the annual groundwater recharge in Thepkasattri watershed using water table fluctuation (WTF) method and chloride mass balance (CMB) method. Besides, seasonal groundwater recharge will be characterized for identifying preferential recharge zones and evaluating the role of streams in groundwater recharge. In addition, vertical electrical sounding will be employed to measure the resistivity of the top layer to model recharge. The integration of these methods is plausible on understanding recharge mechanism in Thepkasattri watershed.

1.3 Research Questions

1. What is the amount of groundwater recharge in the study area?
2. What is the seasonal groundwater recharge variation in the vadose zone?

1.4 Research Objectives

- To estimate groundwater recharge in Thepkasattri watershed, Phuket.
- To predict the spatial distribution of groundwater recharge in Thepkasattri watershed.
- To characterize seasonal recharge mechanism in the vadose zone using time-lapse ERT.

1.5 Research Scopes

Area:

- The study area is located in Thepkasattri watershed in the northern part of Thalang district, Phuket Island, Thailand.

Method:

- WTF and CMB method were used to estimate groundwater recharge.
- Time-lapse electrical resistivity was used to characterize seasonal groundwater recharge.

Duration:

- This research was conducted in eleven months from March 2018 to February 2019.

CHAPTER 2

LITERATURE REVIEW

2.1. Groundwater Recharge

Groundwater recharge is a hydrogeological phenomenon where water from rainfall, lakes, streams, snow melts moves downward to the aquifer. There are two types of groundwater recharge; these are diffuse and focused recharge. Diffuse recharge represents the distribution of recharge in a wide area such as during rainfall while focused recharge represents recharge coming from a point source such as lakes, streams, and depressions (Healy, 2012). Figure 2.1 Groundwater recharge and discharge process in watershed after (Skinner and Murck, 2011).Shows a brief explanation of groundwater recharge and discharge in the watershed. The blue lines represent groundwater flow; these lines move from bottom to top on the stream bed indicating groundwater discharge as base flow. Beside some water is flowing down from the top part (unsaturated zone), indicating groundwater recharge from rainfall and snowmelt. Groundwater moves towards the lowest hydraulic gradient. Thus water comes from the highest gradient recharges groundwater and discharges using pumping from well or naturally as base flow, spring or by joining the sea (Skinner and Murck, 2011).

The amount of water infiltrated to the ground depends on the subsurface hydrogeological parameters and geomorphology of the surface. The main hydrogeological parameters controlling recharge are permeability, hydraulic conductivity, and transmissivity. The geomorphology of the surface includes slope, land use. For example, urbanization and steep slopes increase runoff. These phenomena cause loss of the precipitation reaching the surface of the Earth. Conversely, depression, streams, and forested lands create favorable condition for groundwater recharge and contribute much on groundwater recharge.

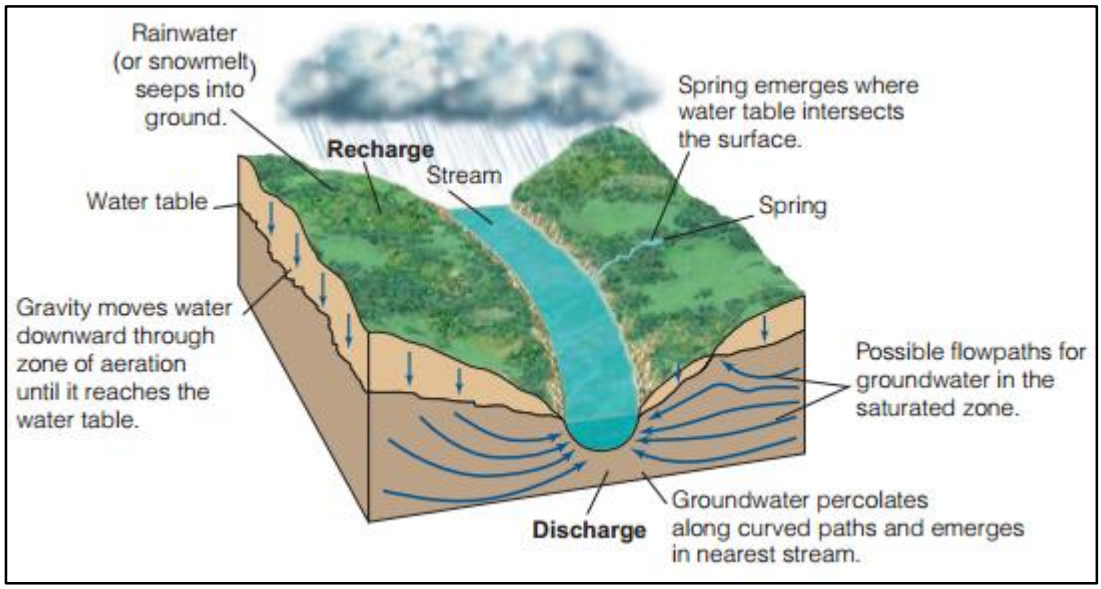

Figure 2.1 Groundwater recharge and discharge process in watershed after (Skinner and Murck, 2011).

2.2 Groundwater Recharge Characterization and Estimation

Israil et al. (2006) used surface electrical resistivity and isotope method to estimate groundwater recharge in the Himalayan foothill region, India. The geology of the area is divided into two formations, the Swalik rocks, and the alluvial deposits. The alluvial deposits composed of sand and gravel layers are the main aquifers of the study area. Thirty-two vertical electrical sounding was taken in every 2 km; then the obtained resistivity was correlated with estimated recharge from tritium tagging method. The result was a linear relationship between the resistivity of the unsaturated zone and the amount of recharge estimated. This is a significant finding and implies the resistivity value of the unsaturated zone increased proportionally with the amount of recharge proved by a high coefficient of determination (R^2=0.97).

Besides, local, seasonal recharge characterization has also been done using electrical resistivity tomography and magnetic resonance sounding. This was done by selecting an experimental watershed along a stream. The electrical resistivity survey was done using Wenner and dipole-dipole electrode configuration. The Wenner array was chosen because it is sensitive to vertical resistivity variation and has a higher

signal to noise ratio, while dipole-dipole is more sensitive to lateral resistivity variation. Therefore, merging of data from different arrays enhance the subsurface imaging and it is a step forward on obtaining a reliable result. The investigation is successful in delineating preferential recharge zones of the watershed. Finally, the stream bed is identified as the main recharge zone for the aquifer beneath the watershed (Descloitres et al., 2008). Groundwater recharge characterization is also done in a depression focused area of Northern America using integrated hydrogeological and geophysical study. Three 2D lines and two 3D grids of electrical imaging were utilized using Wenner and the dipole-dipole electrode array, respectively.

The geochemical data indicate salt accumulation beneath all uplands and leaching beneath depression. The ERI result shows high resistivity value below every larger or smaller depression and low resistivity value below all uplands. This phenomenon indicates there is groundwater recharge beneath all depressions and discharge (accumulation of salt) below uplands. Discharge beneath uplands is controlled by land use change; a large amount of vegetation indicates high discharge and vice versa. Then the result from ERI was compared to geochemical data taken from each piezometer water sample. The correlation shows a good agreement between those two parameters. The result illustrates that ERI is a powerful tool on delineating long term recharge information of subsurface with a short period of acquisition time (Berthold et al., 2004).

Time-lapse electrical resistivity imaging is a widely used technique on delineating seasonal recharge (Arora and Ahmed, 2011; Descloitres et al., 2008; Mojica et al., 2013). Time-lapse electrical resistivity tomography and self-potential for delineating recharge through complex granitic aquifer were done by Arora and Ahmed, (2011). ERI was carried out using the Wenner -Schlumberger array with 48 electrodes. The survey time was divided based on the monsoon period. Thus they gathered 35 tomograms before and after the monsoon. Data processing and interpretation were done using RES2DINV based on smoothness-constrained least-squares method. The result shows a decrease in resistivity value of subsurface after the monsoon, which implies the infiltration of water through the unsaturated zone. The finding was very successful on delineating preferential recharge zones in the study area. Recharge is strongly

controlled by subsurface geology, and the result from time-lapse electrical resistivity was further verified by self-potential and moisture content done at the same time.

Seasonal rainfall infiltration study was also done in Panama Canal watershed using time-lapse ground electrical resistivity. Mojica et al., (2013) used Wenner alpha electrode configuration was used; this method was chosen because it has an advantage in depth of penetration, less sensitive to noise and moderate resolution. A total profile length of 47 m was laid using 48 electrodes with a spacing of 1 m. The field data acquisition was carried in three-time intervals, i.e., dry season, transition season, and rainy season.

Geophysical data obtained during the dry season shows high resistivity value at the top of the profile and lower resistivity value on the right side (Northern part of the study area) of the profile indicating the effect of a nearby stream. This result illustrates the stream has a major role in recharging the watershed aquifer throughout the seasons. In the second survey during the transition period, the profile shows a similar result to the first one, but there is low resistivity value below the surficial soil of a thickness up to 1 m. Finally, the rainy season profile shows a major resistivity decreases in the subsurface starting from the topsoil, indicative of infiltration through the vadose zone is due to the effect of rain. The study establishes a strong relation between vadose zone material resistivity and water infiltration. Therefore, the time-lapse surface electrical resistivity is a powerful method for understanding temporal and spatial characterization of recharge.

2.2.2 The Chloride Mass Balance (CMB) Method

The chloride mass balance (CMB) method is one of the environmental tracer methods used to quantify groundwater recharge. The chloride mass balance theory is based on the assumption that chloride in groundwater is only attributed from the atmosphere through rainfall. Then the amount of recharge is expressed by the equation (Wood and Sanford, 1995):

$$R = \frac{Cl_p}{Cl_{gw}} P \qquad (2.1)$$

Where R is recharge (mm/yr.), P is the amount of precipitation (mm/yr.), Cl_p is weighted average chloride concentration of precipitation (mg/l), and Cl_{gw} is chloride

concentration in groundwater (mg/l) respectively. Recharge estimated using CMB is a point recharge and represents a long-term average recharge. The above equation of CMB is applicable if the area met certain conditions, i.e., 1) There should not be addition or loss of chloride, except chloride attributed by rainfall and 2) there should be no run on or runoff to the aquifer rather than the diffuse recharge. If the runoff is pronounced, the modified equation is strongly recommended (Somaratne and Smettem, 2014; Wood, 1999; Wood and Sanford, 1995). The method was widely applied in semi-arid and arid regions of the world and yield a good result on quantifying recharge. Various authors also recommended the method is best suited in areas with semi-arid to arid climate (Healy, 2012; Scanlon et al., 2002; Wood and Sanford, 1995). However, in recent years few authors implement this method in tropical climate areas, and the result reveals a promising application of CMB method in those areas (Saghravani et al., 2015; Mensah et al., 2014; Hagedorn et al., 2011).

Based on the concentration factor (CF), which is defined as the ratio of the chloride concentration in groundwater and rainfall; it is possible to estimate the evapotranspiration and runoff as well (Aishlin 2006; Ritorto 2007).

$$ET_f = 1 - \frac{Cl_p}{Cl_{gw}} \qquad (2.2)$$

Where ET_f is evapotranspiration, Cl_p and Cl_{gw} are the chloride concentration of precipitation and groundwater respectively.

WTF in combination with CMB was done by various researcher, and the result illustrates recharge estimated using CMB method is higher than WTF. This is because they have used few water level monitoring wells compared with the chloride sampling wells (Afrifa et al., 2017; Saghravani et al., 2014; Takounjou et al., 2011). For instance, recharge estimation is done in Gushiegu (Ghana) and surrounding area was based on 28 groundwater wells for CMB method, and two wells were used for the WTF method. The estimated recharge using WTF is 52.2 mm/yr. to 28.5 mm/yr. and these are between the range of 13.9 mm/yr. to 218 mm/yr. estimated by CMB method. This illustrates when the two methods are used in a similar number of monitoring wells evenly distributed throughout the study area, it can be used to compare WTF and CMB and infer the spatial variation of recharge (Afrifa et al. 2017).

Saghravani et al., (2014) estimate groundwater recharge in the humid climate of Kelantan River catchment in Malaysia. The quantification of recharge was done using CMB (unsaturated zone) method and WTF method from two wells. The mean recharge estimation using WTF for two years is 447 and 319 mm/yr., while the average groundwater recharge using is CMB is 691.8 and 263.3 mm/yr. The result shows different value, which might be due to the fact that WTF is a local scale recharge estimation and CMB is a point scale estimation. However, this is worth noting that the outcomes from these methods in a tropical climate are in agreement with each other. The finding might have been more applicable if it was applied to several evenly distributed monitoring wells.

2.2.1 The Water Table Fluctuation (WTF) Method

Water table fluctuation (WTF) method is widely used and relatively simple method in estimating groundwater recharge. This method utilizes a fluctuation in water head by taking a reference point on the ground surface of the well in relation to time and space (Healy, 2012; Delin et al., 2007; Healy et al., 2002; Scanlon et al., 2002). The WTF method estimates mean recharge in the local base that represents 10 to 1000's square meters. Thus water level fluctuation can be used to ascertain recharge variability caused by climate and land use change (Scanlon et al., 2002). The uncertainties in estimating recharge using WTF is the estimation of specific yield, which varies based on the geology of the aquifer. The equation as given by (Healy, 2012; Scanlon et al., 2002):

$$\Delta S^{gw} = R = S_y \frac{\Delta H}{\Delta t} \qquad (2.3)$$

Where S^{gw} changes in aquifer storage (mm/yr.), R is recharge (mm/yr.), S_y is a specific yield (dimensionless), ΔH changes in water level (mm) and Δt is a change in time during the water level rise (yr.) and the low point of the antecedent recession curve.

This equation assumes the infiltrated water is crossing the water table is added or become part of the storage. ΔH is obtained from the difference of the highest groundwater level recorded and the recession curve extrapolated from the lowest level (Healy and Cook, 2002). The frequency of water level measurement has a major role on the overall recharge estimate. As Morgan and Stolt investigated, recharge estimate

based on weekly water level measurement is underestimated by 33% than recharge estimated based on half an hour interval as cited in (Healy, 2012). The extrapolation of ΔH can be done using the approaches mentioned below:

1. Graphical approach manually extrapolates the antecedent recession curve to obtain ΔH/Δt. This is solely based on the visual assumption of the recession curve would have been followed in the absence of recharge (Delin et al., 2007).
2. Master recession curve (MRC) described by Rutledge is an equation based computation of the antecedent recession curve using a program Fall (as cited in Delin et al., 2007).
3. RISE program described by Rutledge is an approach that simulates the daily rise of water level by comparing with the previous day water level. If the difference is negative, then zero raise is assigned for that day (as cited in Delin et al., 2007).

WTF was successfully applied to estimate weekly and monthly recharge in a rural piedmont environment in Argentina by Cabrera et al., (2016). Hydrogeological data collected by the Department of Geology at the National University of Rio Cuarto. The data used was recorded using a pressure sensor installed in monitoring wells between 01/09/2006 up to 01/09/2009 for 36 months. The data was analyzed for groundwater recharge using Liqo 1.0 software then the estimated recharge was presented and compared with precipitation. Groundwater recharge was estimated based on weekly and monthly data, and the result shows slightly higher in monthly estimate than weekly. However, the overall ratio of recharge and discharge is higher; indicates the aquifer recharge is higher. Finally, the amount of recharge was correlated with the amount of precipitation and no linear correlation was found between them. This occurrence can be due to high runoff as the case in rural Piedmont Argentina or can be due to the low permeability of the unsaturated zone leading to slow percolation of water (Afrifa et al., 2017).

2.3 Electrical Resistivity Method

Electrical resistivity is one of ground geophysical methods used to image the subsurface by injecting an electric current to the ground and measures the potential difference produced by a subsurface body. This method employs four electrodes, two for injecting current and the remaining two are for measuring the potential difference. The principle of electrical resistivity survey governs Ohm's law. The depth of penetration depends on the electrode spacing; when the spacing between the current electrodes increased, the depth of penetration also increased proportionally. The resistivity of a material is defined by (Kearey et al., 2002; Samouëlian et al., 2005):

$$\rho = R\frac{A}{L} \tag{2.4}$$

Where ρ is the resistivity of the material, R is electrical resistance, A is cross-sectional area, and L is the length of the material.

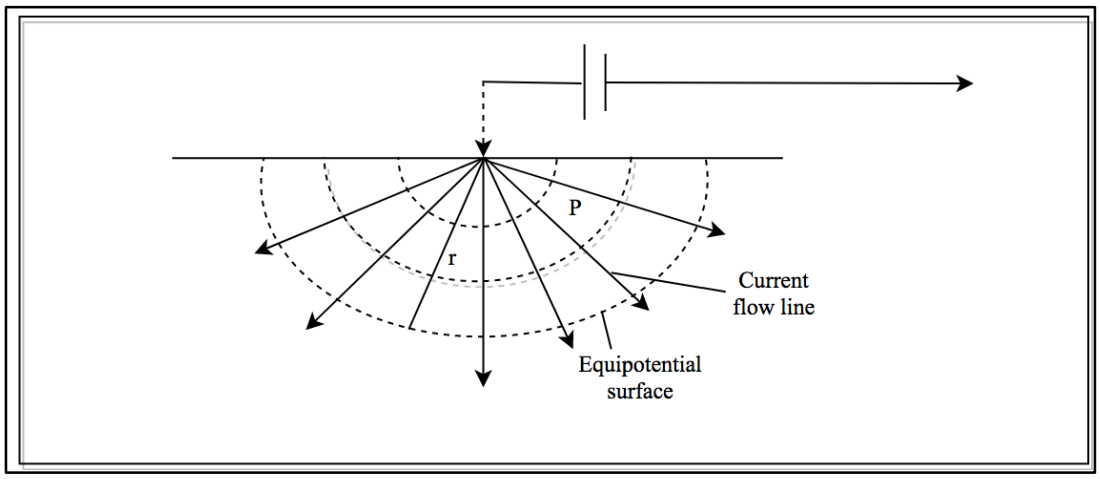

Figure 2.2 Current flow from a single electrode modified from (Kearey et al., 2002).

Considering a single current electrode as shown in Figure 2.2 current flows radially from the source and it is uniform over the homogeneous hemispherical shape. Therefore, the current density for radial directions is given by:

$$J = \frac{I}{2\Pi r^2} \tag{2.5}$$

Where J is current density (A/m^2), I is current (A) and $2\Pi r^2$ (m^2) is the surface of a hemispherical sphere of radius r (m). Then the potential V can be expressed as:

$$V = \frac{\rho I}{2\Pi r} \tag{2.6}$$

Normally measurement of electrical resistivity is done by four electrodes. Two electrodes (A and B) for injecting current and the other two (M and N) for measuring the potential difference. The potential difference measured between the electrodes is given by:

$$\Delta V = \frac{\rho I}{2\Pi}\left[\frac{1}{AM} - \frac{1}{BM} - \frac{1}{AN} + \frac{1}{BN}\right] \tag{2.7}$$

Where *AM*, *BM*, *AN*, and *BN* denotes the geometrical spacing between the four electrodes. Thus, the electrical resistivity is then calculated by:

$$\rho = K\frac{\Delta V}{I} \tag{2.8}$$

Where K is a geometric coefficient that depends on the electrode configuration.

Generally, rocks have high resistivity value, but when water percolates along the fractures and pores the resistivity value drops simultaneously (Figure 2.3). Therefore the resistivity of unsaturated zone of groundwater depends on porosity, while the resistivity of the saturated zone depends on water content (Descloitres et al., 2008). These imply that the resistivity of the subsurface is controlled by lithology, porosity, water content. The electrical resistivity of different materials is given on the table below.

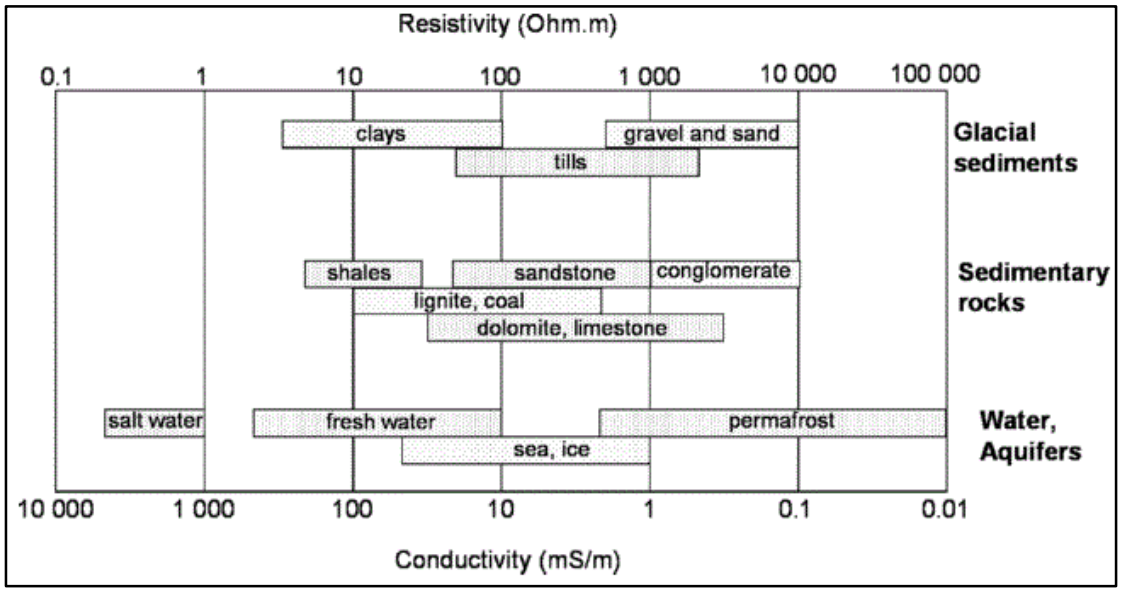

Figure 2.3 The approximate electrical resistivity scope of different materials after (Samouëlian et al., 2005).

Electrical resistivity survey can be done in two ways, namely profiling and sounding. The electrical profiling operates by moving the electrodes along the line with a fixed spacing between the electrodes. While electrical sounding works by fixing the center point of the electrode array and periodically increases the distance between electrodes. Data interpretation from profiling and the sounding survey are mainly qualitative and quantitative respectively. The utilization of these methods depends on the objective of the survey. At this time advanced multielectrode resistivity meter are making 2D and 3D maps of complex geological phenomena in the subsurface. The most common electrode configurations array used for 2D electrical resistivity imaging survey are Wenner, Schlumberger, Dipole-dipole, Pole-pole and Pole-dipole Table 1.1 The most common electrode configuration and geometric factor for 2D electrical resistivity imaging modified after (Samouëlian et al., 2005). Each array configuration has a unique electrode arrangement as well as advantages and disadvantages. Therefore, selection of the array type depends on the target orientation, depth, and layering.

Table 1.1 The most common electrode configuration and geometric factor for 2D electrical resistivity imaging modified after (Samouëlian et al., 2005).

		Electrodes array	K
2D	Wenner	A–a–M–a–N–a–B	2πa
	Wenner-Schlumberger	A–na–M–a–N–na–B	πn(n+1)a
	Dipole-Dipole	A–a–B–na–M–a–N	πn(n+1)(n+2)a
	Pole-Pole	B–x–A–a–M–x–N	2πa
	Pole-Dipole *Forward*	A–na–M–a–N	2πn(n+1)a
	Reversed	M–na–N–a–A	

2.3.1 Schlumberger Electrode Configuration

Schlumberger array is one of the electrode arrangements used for electrical sounding. The method works using four electrodes, the two are potential electrodes, and the other two are current electrodes. In standard Schlumberger electrode configuration, the spacing between potential electrodes kept constant while the spacing between current electrodes changes in every measurement Figure 2.4. The approximate depth of investigation is approximated by dividing the distance between the two current electrodes divided by five.

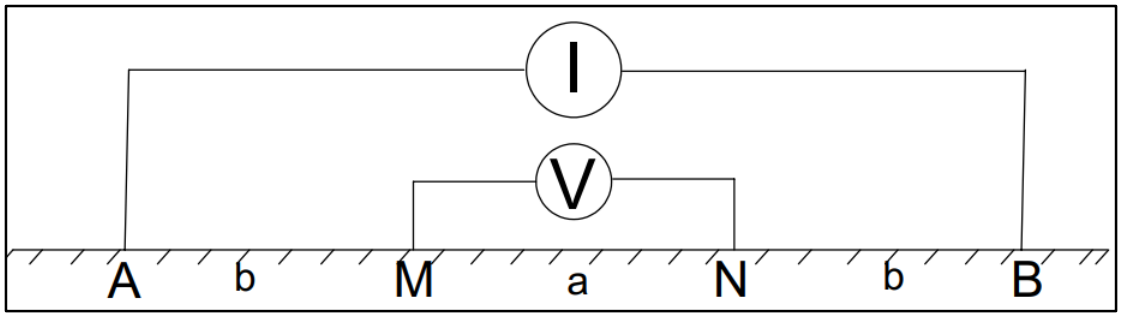

Figure 2.4 Schlumberger electrode configuration.

2.3.2 Time Lapse Electrical Resistivity Tomography (time-lapse ERT)

Time-lapse ERT is a geoelectrical survey, which involves measurement of resistivity variation with time in a fixed position Carey et al. (2017). This technique

was applied by various researchers and yield good result in delineating and characterizing seasonal diffuse recharge (Descloitres et al. 2008; Machiwal et al., 2016; Mojica et al. 2013). This is significant because the method can image the resistivity variation due to water infiltration in the unsaturated zone, which can be used to characterize recharge. However, the major problem with time-lapse ERT is the generation of artifacts during resistivity inversion. Some authors used synthetic data to observe the artifact generation of the different array configuration.

Based on Carey et al. (2017) study artifact produced by dipole-dipole, pole-dipole, Wenner-alpha, Schlumberger and gradient array was evaluated using synthetic data (Table 1.2 Percentage of artifacts generated by different arrays presented by the average, median, maximum and calculated coefficient of variation for the artifact after (Carey et al., 2017).). The result shows the modified pole-dipole array develops least artifact and dipole-dipole is the most susceptible for developing artifact. The study was worth noting as it gives guidance on choosing the appropriate method for time-lapse ERT survey. Clément et al. (2009) also did time-lapse ERT inversion to observe artifact development during leachate injection; the experiment shows symmetrical arrays generate more artifact than the asymmetrical arrays. The result mentioned above is crucial for time-lapse ERT survey and data interpretation, and it can be concluded that asymmetrical arrays and specially pole-dipole is suitable for time-lapse ERT.

Table 1.2 Percentage of artifacts generated by different arrays presented by the average, median, maximum and calculated coefficient of variation for the artifact after (Carey et al., 2017).

Array Type	**$\Delta\rho_{avg}$ (%)**	**$\Delta\rho_{med}$ (%)**	**$\Delta\rho_{max}$ (%)**	**CV (%)**
Dipole-dipole	64.5	64.8	185	66.6
Extended dipole-dipole	71.8	72.3	220.6	70.9
Dipole-dipole gradient	40.3	34.3	141.8	67.8
Gradient	16.8	14.5	47	69.3
Pole-dipole	35.5	23.1	104	86.8
Schlumberger	5.8	4.4	15.3	76.7
Wenner	2.8	2.5	7.6	73.2
Modified pole-dipole	10.0	9.9	24.7	57.6

CHAPTER 3

METHODOLOGY

3.1 Site Description

The sub-district Thepkasattri is located in Thalang district; north east of Phuket. Thepkasattri has an area of around 67 km^2, and according to Anon (2018), the population of Thepkasattri reaches 18,320. The Thepkasattri watershed is bounded by Mesozoic Granitic Mountains in both east and west, and the flat plains are covered by alluvial deposits underlained by the granitic bedrock (Hummel and Phawandon 1967). Tributaries originating from both mountains converge on the plains of Thepkasattri and forms watershed the middle of the floodplain as shown in Figure 3.1. The watershed has an area of 74.3 square kilometers.

The smaller watershed located in north-east has an area of 19.48 square kilometers, and the largest located in the south-west has an area of 54.82 square kilometers. Tributaries from the biggest watershed confluence in the floodplain and makes two main rivers that merge at Choeng Thale estuary and finally drains to the Andaman Sea. The tributaries from the smallest watershed make one prominent river that flows north-east and joins the Andaman Sea through Thepkasattri estuary. Thepkasattri has 27 monitoring wells and more than 42 production wells, for this study 28 wells were used (Appendix I).

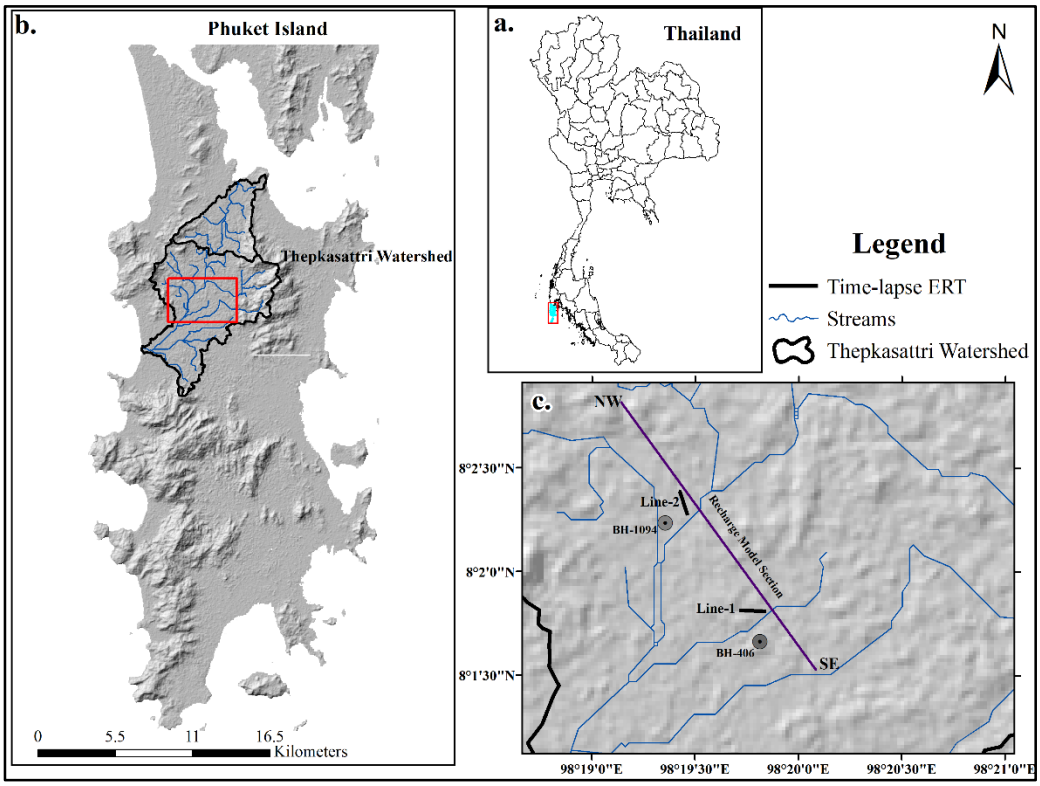

Figure 3.1 Location of the study area and ERT survey lines: (a) Thailand map, (b) Phuket map, (c) Magnified part of the watershed.

Phuket temperature ranges from 23ºC to 33ºC and the maximum temperature recorded in March and April. The amount of rainfall, primarily influenced by South East monsoon reaches the highest precipitation around 400 mm in September and lowest in January around 25 mm. Monthly rainfall distribution from Phuket Airport station is shown in Figure 3.2.

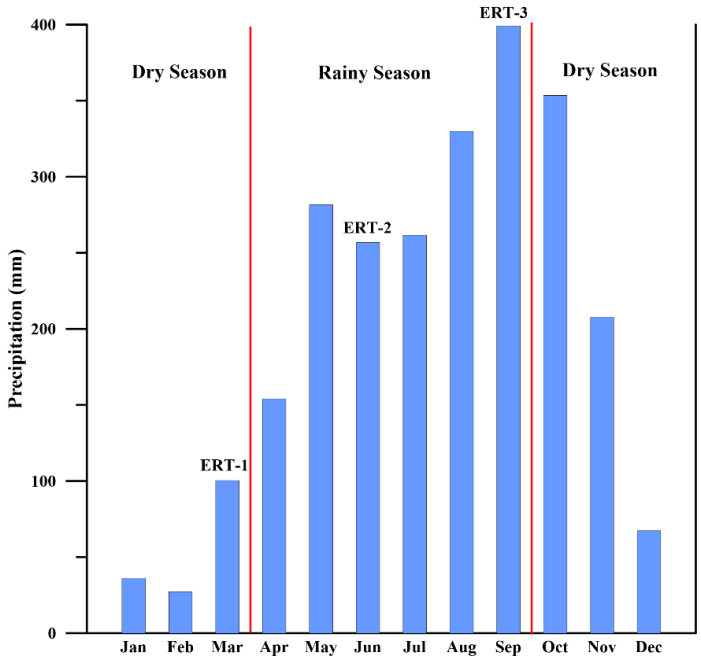

Figure 3.2 Average (1981-2010) monthly precipitation at Phuket Airport Station.

3.1.1 Hydrogeology of the study area

The geology of Phuket is associated with a peninsular orogenic belt. The orogenic belt is characterized by deformed sedimentary and metasedimentary rocks. These rocks are later intruded by younger north trending granitic bodies of Mesozoic age (Figure 3.3). Tertiary to Quaternary sediments of marine, floodplains and river deposits are also irregularly occur throughout the belt (Hummel and Phawandon, 1967).

The intrusive rocks (Kathu Granite) comprises around 75% of the island (Charusiri et al., 1986). The hydrogeology of the aquifer is represented by the unconfined aquifer. The top layer comprises topsoil and weathered rock underlained by fractured granitic bedrock (Alluvial deposit). In Thepkasattri watershed the top layer is alluvial deposit ranges in thickness from 2m to 20m. The weathered rock has a thickness of 6m to 36m, while the granitic bedrock is encountered at depths 28m to 76m. The potential aquifers are the alluvial deposits and weathered and fractured granitic rocks. In this area, the Khao Prathiu Suite and Kata Beach Suite act as potential feeders for the alluvial aquifers in the floodplain.

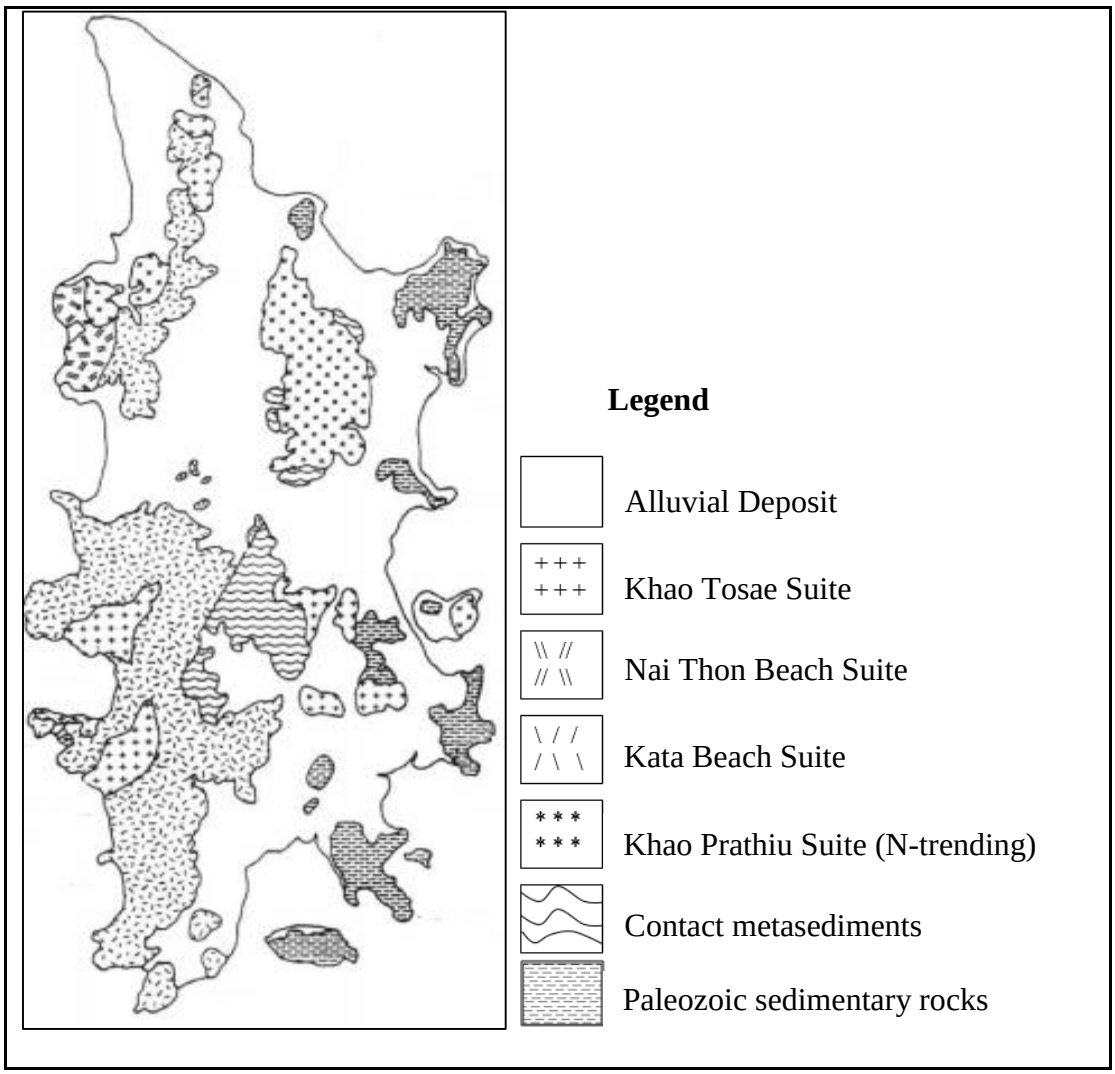

Figure 3.3 Geological map of Phuket by Puttapiban 1984 modified from (as cited in DMR 1989).

Thepkasattri has been identified as high groundwater potential with a shallow water table (Charoenpong et al. 2012). The water table ranges from 1-12 MBGL; eastern catchment has the deepest water table (9-12m), while western catchment has the shallowest water level (1-3m). The middle part has a medium water level between 3.5-8m (Figure 3.4).

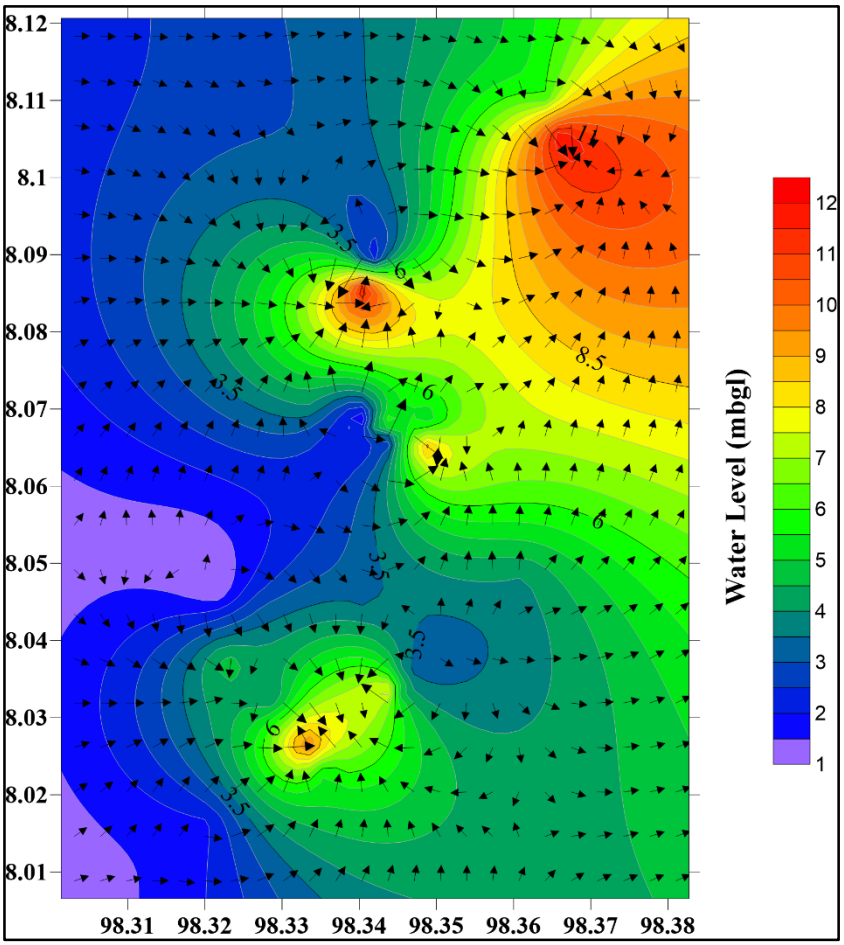

Figure 3.4 The water-table and groundwater flow map of Thepkasattri.

3.2 Preliminary Studies and Research Methodology

Supportive data related to the study area geography and hydrogeology were gathered at the beginning of the study. Satellite image and Phuket shapefile are employed to outline the study area and locate wells in the study area. The watershed area was outlined from the digital elevation model (DEM), and the geological section of the aquifer was analyzed from borehole data.

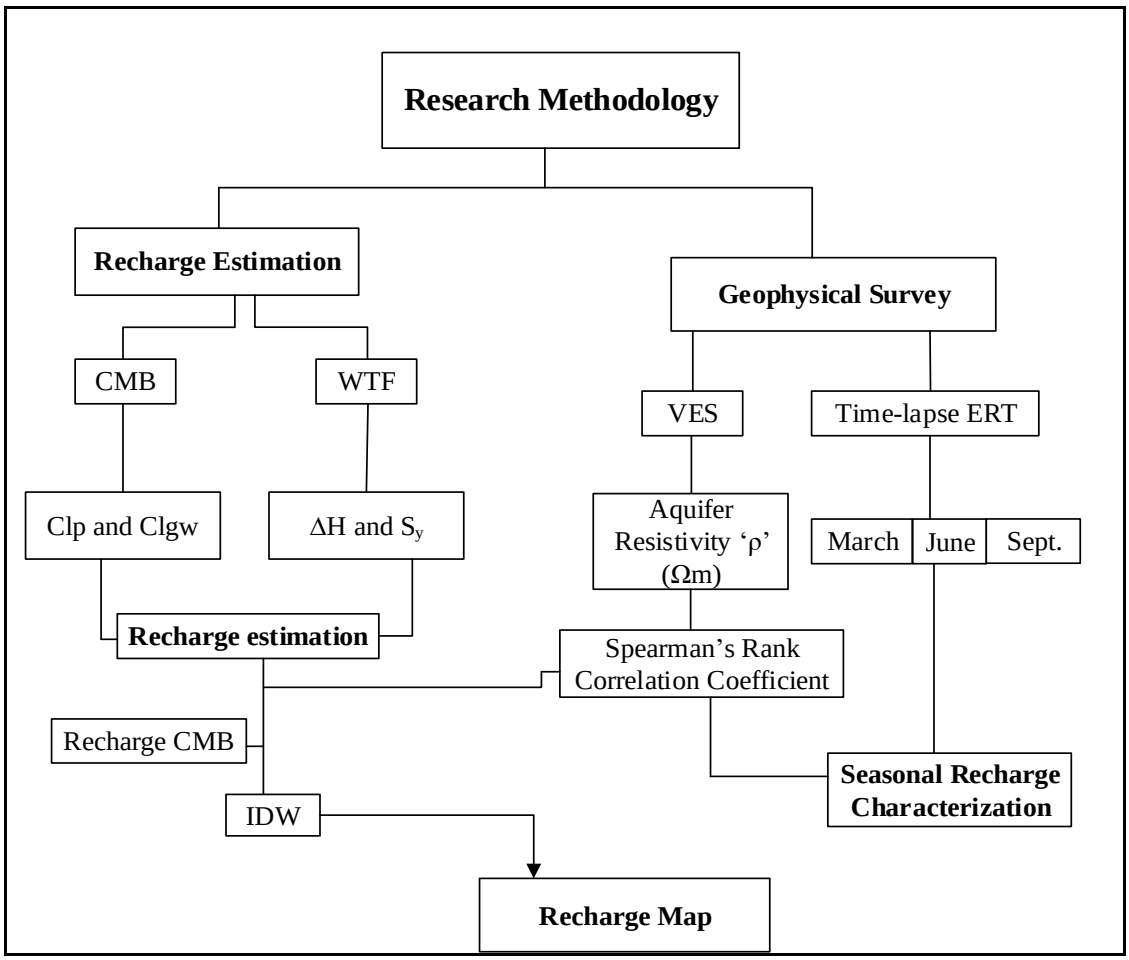

Figure 3.5 Research methodology flow chart.

Summarized flow chart of the methodology section is shown in Figure 3.5; there are two principal objectives of this research; these are recharge characterization and estimation. Recharge estimation that was done using WTF and CMB method. The second part is recharge characterization was done using time-lapse electrical resistivity imaging in three-time divisions (Figure 3.2). Finally, spatial recharge distribution was predicted using the Inverse Distance Weight (IDW) interpolation technique (section 3.5). Historical groundwater level data of Thepkasattri was used for the application of the WTF method. The unpublished groundwater level data is provided by the Department of Groundwater Resources of Thailand (DGR). Details of the flow chart is explained in the following sections.

3.3 Recharge Estimation using Chloride Mass Balance (CMB) Method

Groundwater samples from 28 wells were collected for chloride content analysis. The selection method is based on the availability of wells and spatially representation of the whole watershed. Majority of the wells are monitoring wells, and eight wells are production wells (GW02-GW34), all are drilled by the Department of Groundwater Resources of Thailand (Figure 3.6). In addition, fifteen rainfall samples (RW01-RW15) were collected every month from April to October for determining the average atmospheric wet chloride deposition. The standard sampling procedure is given by the U.S. Geological Survey (2015) and Grynkiewicz et al., (2003) was followed for the collection of groundwater and rainwater samples. All samples were collected using 500ml and 1000ml polyethylene bottles.

The electrical conductivity of each sample was measured using a portable Ohaus (ST300C) and Hanna (HI9813-6) instrument. Then the water samples were sent to Environmental Lab in Phuket Rajabhat University for chloride concentration determination. The titration method was used to determine the level of chloride in each water sample. The titration method is a process of determining a substance by adding a measurable amount of standard solution. In the sample analyzed silver nitrate is added as a standard solution and reacts with Chloride. Then the concentration of the chloride ion is determined by the stoichiometry of the reaction. As the silver nitrate solution is slowly added, a precipitate of silver chloride forms.

$$Ag^{+}_{(aq)} + Cl^{-}_{(aq)} \Longrightarrow AgCl_{(s)}$$

The endpoint of the titration method occurs when all the chloride ions are precipitated. This is indicated by the reaction of extra silver ions with chromate ions of the indicator, potassium chromate, to form a red-brown precipitate of silver chromate.

$$2Ag^{+}_{(aq)} + CrO_4^{2-}{}_{(aq)} \Longrightarrow Ag_2CrO_{4(s)}$$

The measurement error of the titration method is +/-0.1mg/L. Although the analysis was done by another laboratory, the quality of the laboratory procedure was evaluated using a single-blind experiment where a duplicate sample was sent to verify the analysis procedure. The measurement accuracy was not checked through a

standard sample, but the laboratory is certified according to ISO/IEC 17025 (Accreditation number: 14T110/0192). Therefore, the accuracy of measurement is believed to be at the standard level (Thai Industrial Standards Institute (TISI)).

Weighted average chloride content of rainwater was computed to determine wet chloride deposition. Then groundwater recharge in mm/yr. was calculated using the CMB formula given in equation (2.1).

Furthermore, possible evapotranspiration of each sampling point and the average evapotranspiration for the whole watershed was computed using the concentration factor given in equation (2.2).

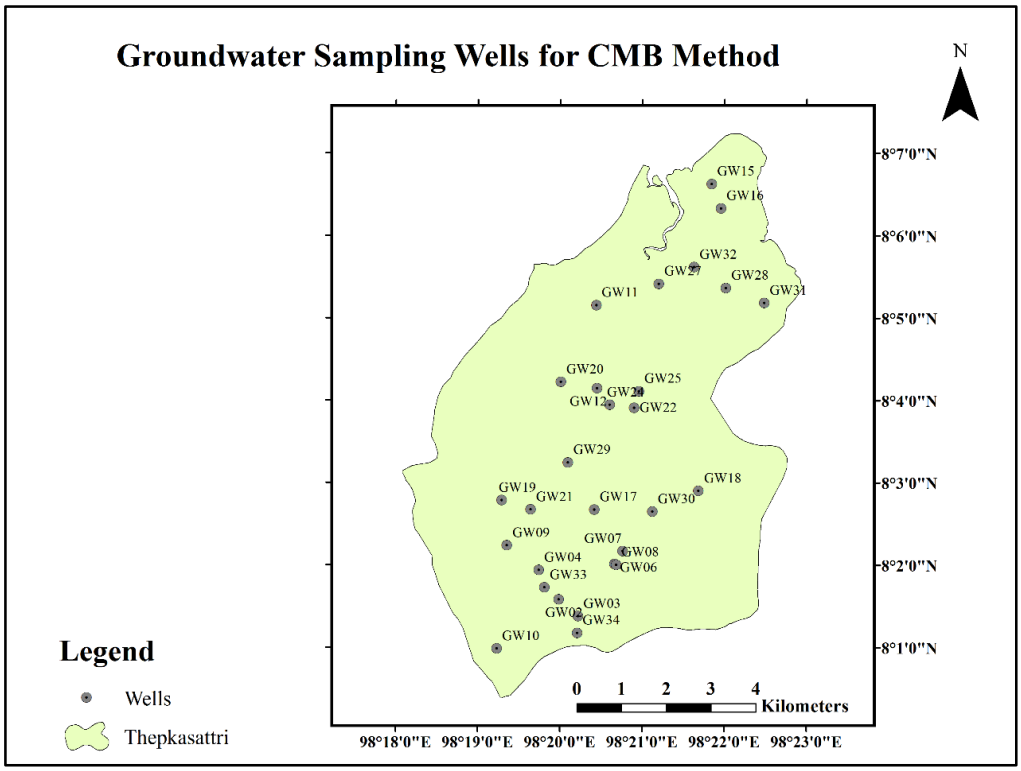

Figure 3.6 Showing the location of groundwater sampling wells.

3.4 Recharge Estimation using Water Table Fluctuation (WTF) Method

Hourly groundwater level data from 2012 to 2015 was used for applying the WTF method to estimate recharge. The unpublished groundwater level data is provided by the Department of Groundwater Resources of Thailand (DGR). The

groundwater level data were recorded by PT2X sensor. The PT2X sensor measures pressure and temperature with integrated data logging collects up to 520,000 records. The frequency of measurement was on an hour, and it was collected from 2012 to 2015. The measurement doesn't cover each month of the year. In 2012 the data recorded from July to September 2013 from March to August, in 2014 from November to December and for 2015 from January to December. The groundwater level data was plotted on groundwater well hydrograph so that the recession curve can be inferred through a graphical approach.

The graphical approach was used to obtain ΔH. In a graphical approach the antecedent recession curve is extrapolated manually. The specific yield of the aquifer is estimated from standard values given by Johnson (1963) and from literature review from the same aquifer geology in Malaysia (Saghravani et al., 2015). Then annual recharge was computed from the above-mentioned parameters using WTF formula given in equation (2.3).

3.5 Mapping of Groundwater Recharge in Thepkasattri

Finally, the point scale recharge estimated from the above methods was interpolated to predict spatial variation of recharge using the geostatistical tool the IDW. The IDW is considers the interpolation based on the distance of measured points from the point needed to be interpolated (equation 3.1). Therefore, in IDW the data close to unsampled point has greatest weighting value. This interpolation technique was done using Arc Map software. Then the predicted recharge map was compared to a land cover map of Thepkasattri. The objective of the comparison is to observe the effect of land use and cover change in the spatial distribution of groundwater recharge.

$$Z_p = \frac{\sum_{i=1}^{n} (\frac{Z_i}{d_i^p})}{\sum_{i=1}^{n} (\frac{1}{d_i^p})} \qquad 3.1$$

Where Z_p is the value to be predicted for location S_o, N is the number of measured sample points surrounding the prediction location, Z_i is the observed value at the location S_i, and p the power of the interpolation function.

3.6 Electrical Resistivity Survey

3.6.1 Vertical electrical sounding (VES)

The location of the VES survey is chosen based on the location of chloride sampling wells and the availability of space as well (Figure 3.7).

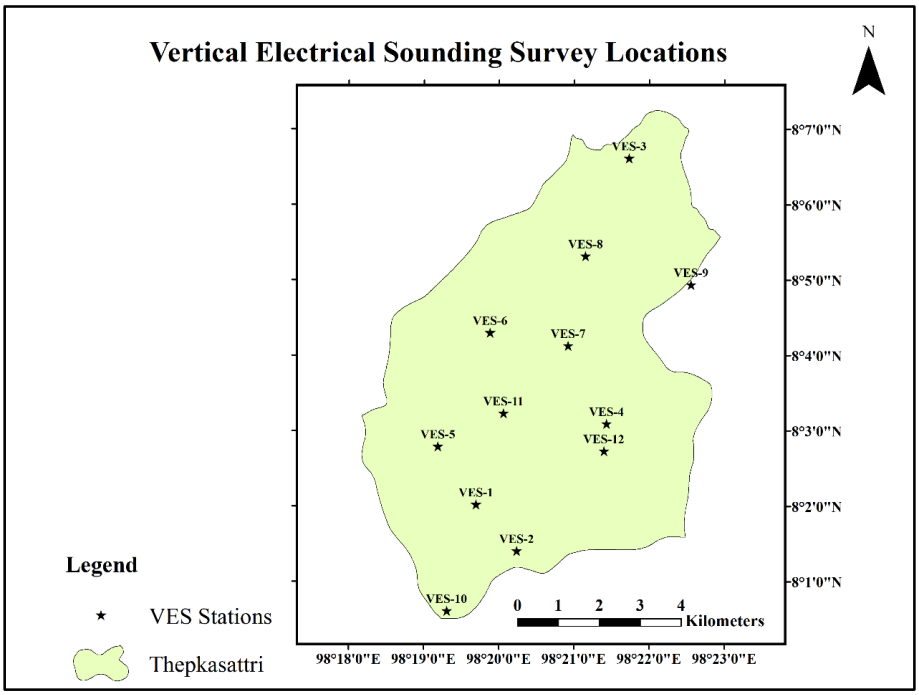

Figure 3.7 Shows the location of the vertical electrical sounding survey.

The vertical electrical sounding was carried out using AGI SuperSting R2. The electrode configuration chosen for this survey is Schlumberger array with maximum and minimum electrode spacing 98 m and 1.5 m respectively (Table 3.1). The estimated maximum depth of penetration is 20m. The spacing was chosen based on the top layer thickness and groundwater level data analyzed from well logging. Then the resistivity of the aquifer was extracted from VES curve (Appendices II).

Table 3.1 Vertical electrical sounding (VES) survey plan.

Recording	MN/2	AB/2	Recording	MN/2	AB/2
1	0.5	1.5	8	1	17
2	0.5	3.5	9	1	21
3	0.5	5.5	10	1	29
4	0.5	7.5	11	1	35
5	0.5	9.5	12	1	41
6	1	9	13	1	47
7	1	13	14	1	49

3.6.2 Seasonal groundwater recharge characterization using time-lapse ERT

The location of geophysical survey lines was in the south-west of the study area; chosen based on the path of the two streams crossing the study area and the availability of space as well (Figure 3.8). The line was oriented perpendicular to the stream drainage to investigate the contribution of the stream on groundwater recharge.

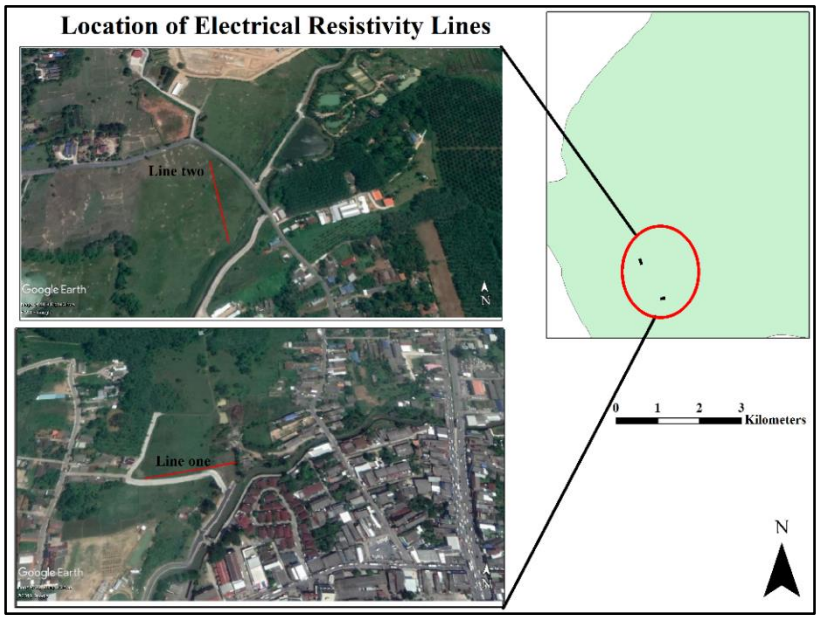

Figure 3.8 Location of the electrical resistivity survey for line one and line two. Left satellite image from Google Earth.

The electrical resistivity imaging was carried out using AGI SuperSting R2 with 56 electrodes. Due to the limitation of space for infinity remote electrode in the Pole-Dipole array, the time-lapse ERI survey was done using the Wenner array. The electrode spacing was 2.5m in line one and 3m in line two. The total profile length was 137.5m and 155m for both lines respectively. The estimated depth of penetration using Wenner and Dipole-dipole array is 27.5m and 31m respectively (Table 3.2).

I. First Phase

The first phase of electrical resistivity imaging (ERI) was done during the dry season to in March. This survey provides a cross-sectional view of the subsurface of the study area. This data was used as a monitoring profile for the proceeding electrical resistivity surveys during the wet season.

II. Second Phase

The second phase was at the middle of the rainfall time in June. The electrical resistivity survey on this date was aimed at observing the recharge phenomena of the vadose zone during the beginning of the rainy season. The purpose of this survey is to observe the resistivity variation of the vadose zone with respect to the dry season.

Table 3.2 Electrode configuration and survey plan for time-lapse ERI.

ERT	Survey Date	Electrode configuration	Electrode Spacing		Profile length	
			Line-1	Line-2	Line-1	Line-2
I-Phase	March	Wenner Array	2.5m	3m	137.5m	165m
II-Phase	June	Wenner Array	2.5m	3m	137.5m	165m
III-Phase	September	Wenner Array	2.5m	3m	137.5m	165m

III. Third Phase

The last phase was during the end of the wet season, and the data acquisition was in September. Finally, the data from phase II and phase III was inverted

using time-lapse inversion by fixing phase I as a background profile. Then the difference in inverted resistivity was presented as a percentage ranging from 100% to -100%.

3.6.3 Electrical Resistivity Data Inversion and Interpretation

The data from the electrical resistivity survey was processed using EarthImager 1D and 2D inversion software. The software is developed by the Advanced Geoscience Incorporation (AGI) (Advanced Geoscience Incorporation, 2009). In this study, the inversion model chosen to invert the measured resistivity value is the least square inversion method (L2). This model applies the L2 norm and "minimizes the sum of squares of the spatial changes in the model resistivity and the data misfit". The data inversion tries to minimize the root mean square error between the measured apparent resistivity value and calculated resistivity value (Loke et al., 2003).

The electrical resistivity tomography is interpreted based on well log data of the study area provided by DGR. There are two boreholes in the study area, BH-402 was used for line one and BH-1094 was used for line two. In addition, helpful field data observation was noted to enhance the interpretation.

3.7 Recharge Estimation Evaluation among CMB, WTF and VES Method

The quantified recharge estimated using WTF and CMB will be evaluated to observe the overall spatial and temporal variation of recharge in the study area. In most previous work recharge estimated using WTF is less than recharge estimated by CMB. This can happen because WTF is local scale estimation while CMB is point scale estimation. The number of wells used to perform both methods also have a significant effect on final recharge estimation. In addition, the Spearman's rank correlation coefficient is used to evaluate association among the variables recharge, groundwater chloride, groundwater resistivity and aquifer resistivity. For this purpose, a total of twelve VES station was selected in proximity with groundwater sampling well. The inverted resistivity of the aquifer is used for applying Spearman's correlation. In addition, recharge computed using the CMB method and pore water resistivity converted from electrical conductivity was used. Finally, the Spearman's rank

correlation coefficient was computed to evaluated the association using the following equation.

For a sample of size *n*, the n raw scores X_i, Y_i are converted to ranks x_i, y_i and r_s is written as,

$$r_s = 1 - \frac{6\sum d_i^2}{n(n^2-1)} \qquad 3.2$$

Where $d_i = x_i - y_i,$ is the difference between ranks. *n* is the number of pairs (Lin et al. 2017). The numerical value of r_s ranges between -1 and +1. The strength of the correlation can be described through the following guide Table 3.3.

Table 3.3 Guide for describing the Spearman's rank correlation coefficient (Lin et al. 2017).

Spearman's rank correlation coefficient (r_s)	**Description**
$0 \leq \lvert r_s \rvert < 0.2$	Very weak
$0.2 \leq \lvert r_s \rvert < 0.4$	Weak
$0.4 \leq \lvert r_s \rvert < 0.6$	Moderate
$0.6 \leq \lvert r_s \rvert < 0.8$	Strong
$0.8 \leq \lvert r_s \rvert \leq 1$	Very strong

CHAPTER 4

RESULTS AND DISCUSSION

4.1 Groundwater Recharge Estimation

4.1.1 Recharge Estimation using the Chloride Mass Balance (CMB)

Groundwater recharge using the CMB method was computed using 28 groundwater (G02-G35) and 15 rainwaters (RW01-RW15) samples (Table 4.1 and Table 4.2). The weighted average chloride contribution from precipitation is 9.3 mg/l with a standard deviation of 1.9 mg/l (Table 4.1). The chloride content of groundwater varies from 16 to 52 mg/l, with average and standard deviation of 20.5 and 6.8 mg/l respectively (Table 4.2). The electrical conductivity of groundwater samples is generally low, ranges from 51 to 478 µS/cm, with an average of 175 µS/cm. The low electrical conductivity of groundwater suggests groundwater is fresh and has not geochemically evolved (Afrifa et al. 2017; Yidana and Koffie 2014).

Table 4.1 Physico-chemical parameters of rainwater.

Sample ID	EC µS/cm	Cl^- mg/L	Sample ID	EC µS/cm	Cl^- mg/L
RW-01	13.84	9	RW-09	47.9	12
RW-02	35.2	9	RW-10	43.6	9
RW-03	3.39	8	RW-11	17.33	11
RW-04	1.39	6	RW-12	10.46	12
RW-05	14.11	10	RW-13	3.52	11
RW-06	10.01	7	RW-14	1.03	11
RW-07	24.6	12	RW-15	1.48	10
RW-08	1.82	8			

The CMB method is applicable if the chloride contribution is only from precipitation. In Thepkasattri there is no significant source of chloride other than precipitation; most of the land use is covered by rubber plantation, forest, and crops. The contribution of chemicals from agriculture are mainly nitrate and pesticide (Tirado et al., 2008). Chloride contribution from weathering of rocks is not considered since the geology of the study area is consisting of weathering product of granite. There is no major source of chloride from seawater intrusion or industry as well. The study area is far (around 3.5km) from the coast and the EC and chloride concentration of groundwater sample support this assumption. Annual precipitation in the study area is highly variable. Thus an average over 30yrs was used for the application of CMB method. Then recharge was estimated using the ratio of weighted-average chloride in rainwater to chloride in groundwater multiplied by 30-year (1981-2010) average annual rainfall of 2,475 mm. Phuket rainfall varies from year to year. Thus an average of 30 years was used.

Based on the CMB equation recharge in Thepkasattri varies from 443 to 1,439 mm/yr. with an average value of 1,172 mm/yr. (Figure 4.1). The average recharge accounts for 47% annual precipitation. The volume of recharge in was computed by multiplying with the area Thepkasattri. Hence, mean annual recharge represents a volume of 78.52 hm^3/yr. There might be some uncertainty with recharge estimated associated with obtaining mean chloride contribution from precipitation. Most reliable data of rainfall chloride can be obtained from long and continuous measurement chloride from rainfall. However, this data is not available in the study area, and there is no precipitation chloride database in Phuket.

Table 4.2 Physico-chemical parameter of groundwater in Thepkasattri.

Well-ID	EC (µS/cm)	Cl^- (mg/L)	Well-ID	EC (µS/cm)	Cl^- (mg/L)
GW02	478	27	GW19	74	17
GW03	292	16	GW20	219	18
GW04	247	19	GW21	100	21
GW06	267	20	GW22	52	20
GW07	266	23	GW24	175	18
GW08	267	22	GW25	279	20
GW09	114	18	GW27	114	27
GW10	464	52	GW28	51	18
GW11	75	20	GW29	97	20
GW12	117	20	GW30	64	17
GW15	86	17	GW31	169	26
GW16	73	19	GW32	290	16
GW17	340	18	GW33	44	19
GW18	103	17	GW34	101	16

Based on the concentration factor, the study area has an average concentration factor of 0.47 (47%) indicates that evapotranspiration has caused more than one times to increase in chloride concentration. Therefore, 0.53 (53%) of rainwater has evapotranspired. Ministry of Agriculture and Cooperatives of Thailand has done evapotranspiration estimation from the weather station in the study area (Phuket airport) using the Penman-Monteith method (Table 4.3). The maximum evapotranspiration occurs in March with the average value 4.58 mm, and minimum evapotranspiration recorded in October (3.19 mm). The report shows evapotranspiration results in the loss of 1416.67 mm of annual rainfall; this represents 57.24% of annual precipitation (Ministry of Agriculture and Cooperatives 2011). Considering some uncertainty associated with the location of the measurement, sample representation (spatial and temporal) and measurement error, the evapotranspiration estimated using the concentration factor agrees with the Penman-Monteith method.

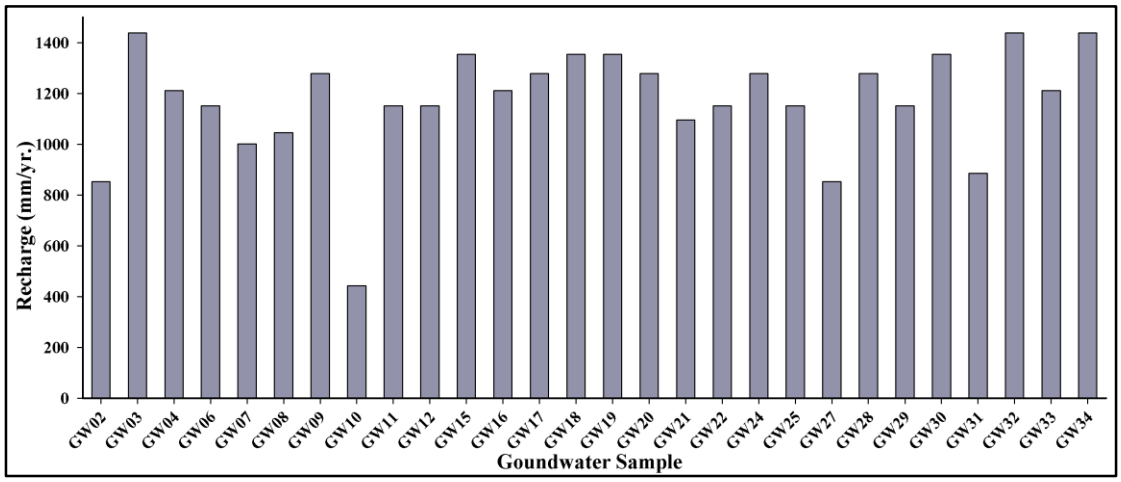

Figure 4.1 Bar chart showing the groundwater recharge rate at each sampling point.

In Thepkasattri there is no river or major stream drainage, and most land covers are covered by forest and rubber plantation. Thus runoff is low, and evaporation and transpiration are most pronounced. Therefore, it is assumed that most of the precipitation is lost in the form of evapotranspiration.

Table 4.3 Evapotranspiration estimation using Penman-Monteith from the station after (Ministry of Agriculture and Cooperatives 2011).

Month	**Min Temp** (^oC)	**Max Temp** (^oC)	**Humidity** (%)	**Wind** (Km/day)	**Sun** (hrs.)	**Radiance** ($MJ/m^2/day$)	**ET_f** (mm/day)
Jan.	22.6	32.1	76	160	6.4	17.3	4.04
Feb.	22.8	33.1	74	151	6.4	18.3	4.37
Mar.	23.4	33.6	76	147	6.5	19.4	4.58
Apr.	24.2	33.4	80	125	6.1	18.9	4.36
May	24.7	32.2	82	151	5.0	16.8	3.93
Jun.	24.9	31.7	82	200	5.0	16.4	3.93
Jul.	24.6	31.3	82	205	5.0	16.5	3.92
Aug.	24.9	31.2	82	245	3.7	14.9	3.78
Sep.	24.2	30.7	84	191	3.6	14.8	3.52
Oct.	23.8	30.8	86	129	3.5	14.1	3.19
Nov.	23.5	31.1	83	116	4.6	14.9	3.32
Dec.	22.9	31.2	79	156	5.8	16.0	3.67

4.1.2 Recharge Estimation using the Water Table Fluctuation (WTF)

As shown in the figure below the hydraulic head measurement was not complete record throughout the calendar year except for the year 2015. In 2012 the data ranged from July to September 2013 from March to August, in 2014 from November to December.

In 2012, 2013 and 2015 the well hydrograph reaches a maximum level between August and September. The exception is for 2014, and this might be due to a lack of data to represent the whole trend of the well hydrograph (Figure 4.3). The highest water level in August and September is connected with rainfall distribution of the area (Figure 3.2). However, there is a small water level rise in the dry season as well. This is associated with delayed drainage and a small amount of precipitation recorded in those months. Thus based on the trend of the well hydrograph it is possible to establish the hydrologic year of the aquifer. The hydrologic year extends from 15 of September to 14 of the succeeding year September.

Recharge estimation using the WTF method is done using equation 2.1. The change of water level per unit time was computed using the difference between the highest water level and the extrapolated antecedent recession curve. The extrapolation was done manually by following the graphical approach (Delin et al. 2007). The specific yield of the aquifer was taken from the standard values given by Johnson (1963). For a more reliable estimation of specific yield, literature was referred for similar aquifer geology in Malaysia. The specific yield of alluvial deposit in Malaysia from 0.11 to 0.23 (Saghravani et al., 2015). Based on the well log data of the well provided by DGR the aquifer is composed of alluvial deposit (gravel, very fine pebble poorly sorted with rock fragments and clay). The second layer underlained the alluvial deposit is granitic bedrock; lithologically composed of feldspar, biotite, and quartz.

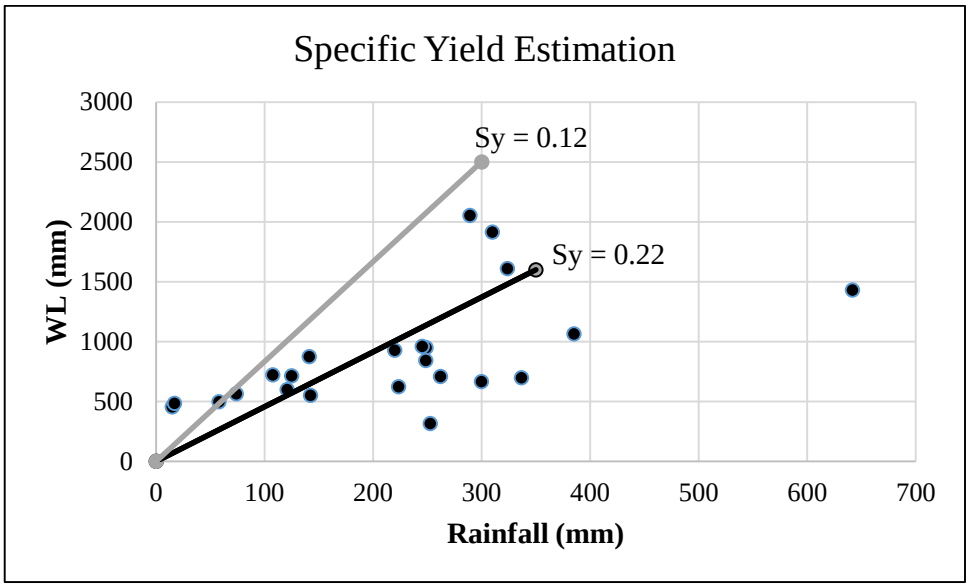

Figure 4.2 Estimation of specific yield from the relationship between rainfall and water level.

Moreover, a graphical method proposed by Varni et al. (2013) was used to obtain specific yield. In the graphical procedure, the specific yield is determined by drawing straight envelope line drawn on precipitation versus water level rise scatter plot. The straight envelope line is drawn above all the measured points gives a maximum value. The method is most reliable for historical WTF data of many years. However, this is not available in the study area. Therefore, the available data (23 measurement points) were used. The scatter plot shown in Figure 4.2, from the straight envelope line drawn from the origin, the line has a slope of five. Thus the inverse of the slope, which is the specific yield of 0.12-0.22. This is within the range taken from standard values and literature review of similar geology (0.16-0.23). Therefore, based on the above information the specific yield value 0.12-0.22 used as the upper and lower limit of uncertainty to estimate recharge using WTF method.

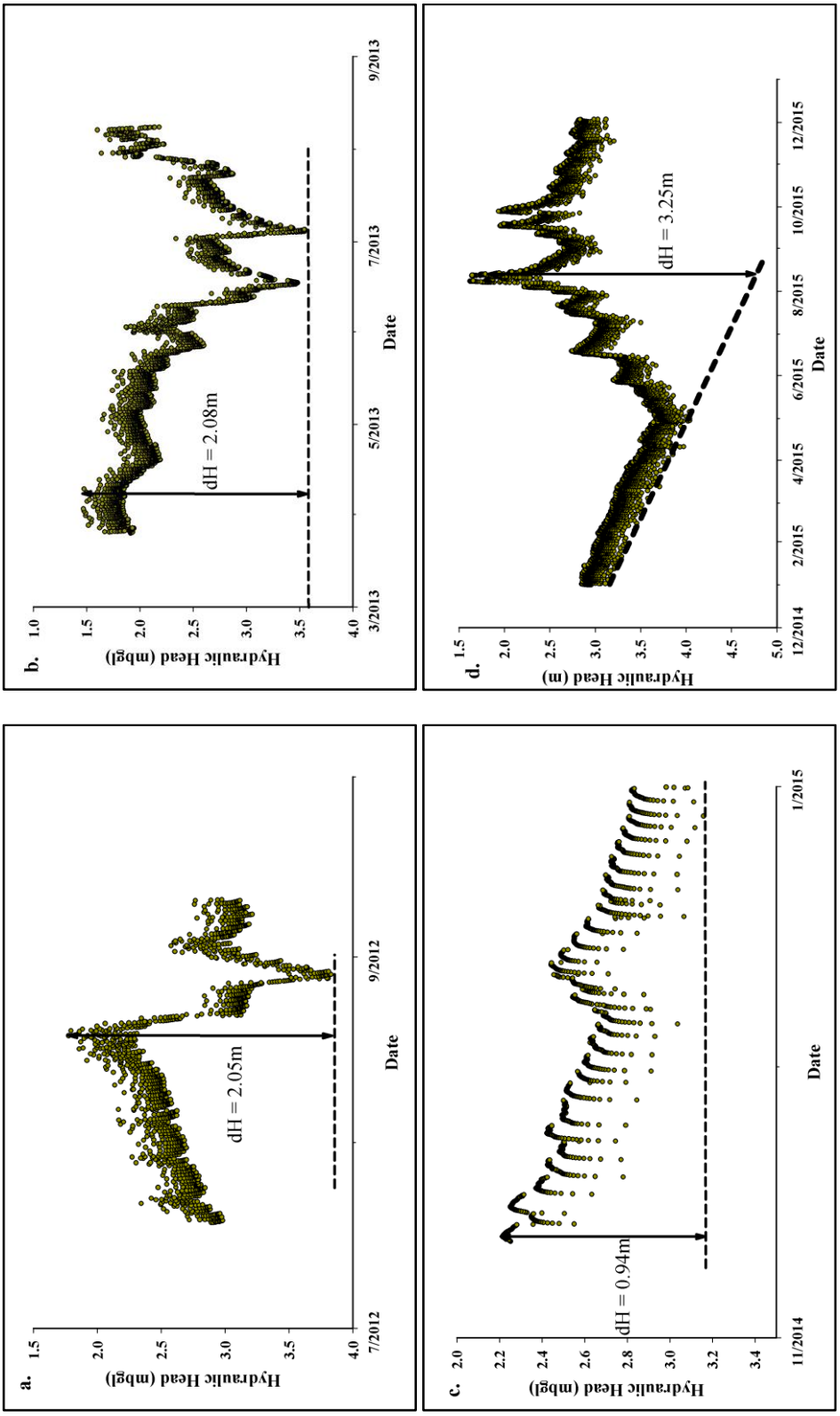

Figure 4.3 Well hydrograph is showing water level changes from 2012 to 2015.

Based on the WTF method, the calculated mean recharge for the year 2012, 2013, 2014 and 2015 were 349 mm/yr., 354 mm/yr., 160 mm/yr. and 552 mm/yr. respectively (Table 4.1). The estimated recharge except 2014 represents between 16%-25% of annual rainfall. The recharge estimated using the WTF method falls in the range of 18%-58% of annual recharge computed using the CMB method. Both methods cannot be compared to each other since the CMB method is point scale while the WTF is local scale recharge estimate, that represents hundreds and thousands of square meters.

An important question associated with the application of the WTF method is the underestimation of recharge. This underestimation of recharge is attributed due to insufficient water table fluctuation data that represent a complete calendar year as the case in 2012, 2013 and 2014. This gap of data caused the underestimation of the extrapolation of the antecedent recession curve. Hence, the antecedent recession curve for 2012-2014 is extrapolated based on the corresponding hydraulic head fall in the rainy season. In addition, the number of monitoring wells used for the application of the WTF is insufficient to represent the study area.

Table 4.4 Recharge estimated using the water table fluctuation method.

Year	**ΔH (mm)**	**S_y**	**Mean Recharge (mm/yr.)**	**% Annual Rainfall**
2012	2050	0.12-0.22	348.5	15.93
2013	2083	0.12-0.22	354.1	16.18
2014	940	0.12-0.22	159.8	7.30
2015	3250	0.12-0.22	552$\pm$34	25.23$\pm$1.5

The relationship between precipitation and hydraulic head variation is useful to deduce the temporal variability of groundwater recharge. Thus a correlation was done to observe the relationship between the hydraulic head and the amount of rainfall in the area. The highest rainfall is recorded between August and mid of October

in all years except 2012. In 2012 the highest rainfall was recorded between April and May. The trend of precipitation corresponds with the well hydrograph.

Furthermore, since 2015 well hydrograph is complete throughout the calendar year, an association plot is drawn with the mean monthly precipitation on that year. As shown in Figure 4.4 water level rise in well hydrograph has relationship to the amount of rainfall. The highest precipitation (385 mm) was recorded in August so as highest water level rise (1.6 mbgl).

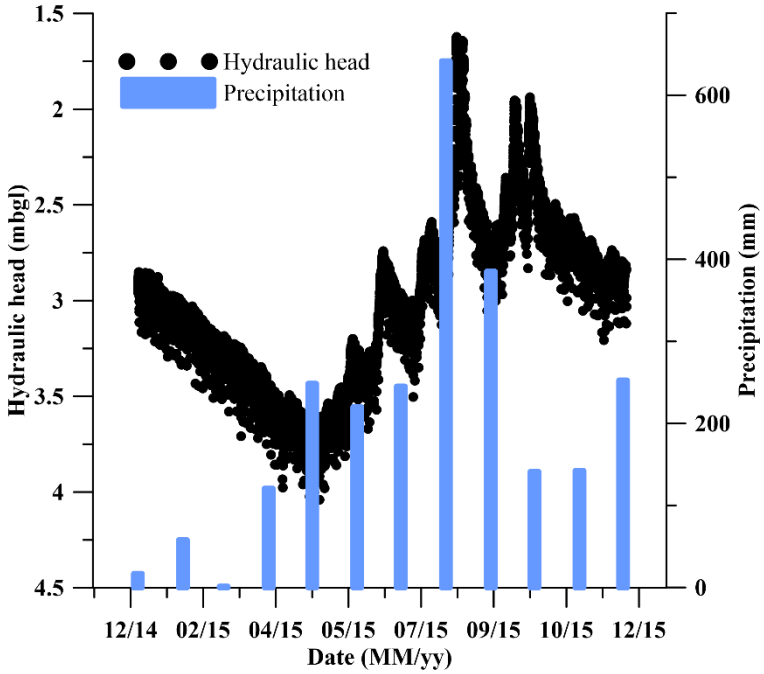

Figure 4.4 Annual rainfall versus water table fluctuation for the year 2015.

4.1.3 Spearman's Rank Correlation Coefficient

The Spearman's rank correlation coefficient is important to evaluate association among monotonic functions. Therefore, to determine the association among recharge, groundwater chloride, water resistivity and aquifer resistivity a Spearman's correlation coefficient done by ranking each value (Table 4.5).

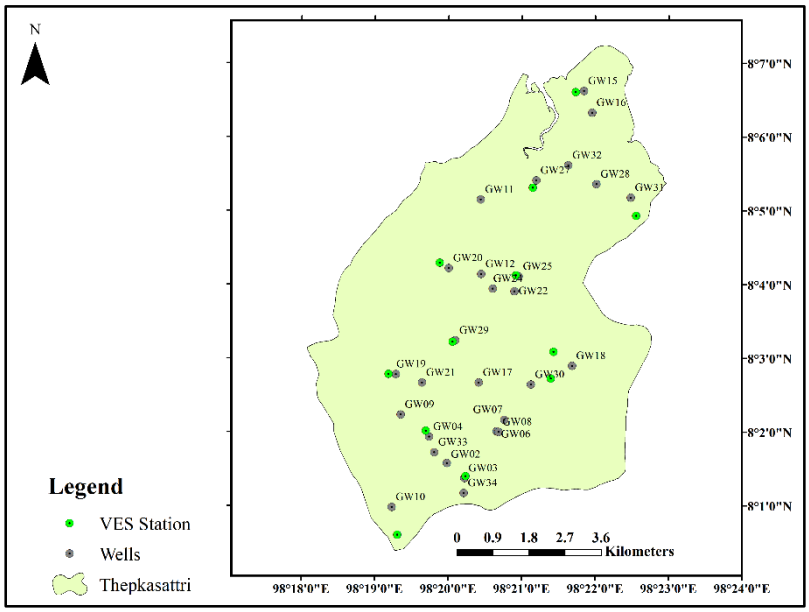

Figure 4.5 Map Showing the location of sampling wells and VES stations.

The correlation test was done for twelve selected locations as shown in Figure 4.5 Figure 4.5 Map Showing the location of sampling wells and VES stations. (See Appendix II for VES curves). The Spearman's rank correlation value along with description is shown in Table 4.6.

Table 4.5 Ranking orders for chloride in groundwater (Cl_{gw}), recharge, groundwater resistivity (ρ_{gw}) and aquifer resistivity.

Cl_{gw}		Recharge		ρ_{gw}		Aquifer resistivity	
mg/L	Rank	mm	Rank	Ωm	Rank	Ωm	Rank
19	4.5	1211	8.5	40.57	10	100	8
27	1	853	12	87.72	6	84	10
19	4.5	1211	8.5	136.99	2	87.5	9
17	10	1354	3	96.71	5	113.5	6
17	10	1354	3	135.78	3	135.5	3
18	7	1279	6	57.14	9	169	2
20	3	1151	10	35.91	11	60.21	12
18	7	1279	6	85.47	7	131	4
26	2	885	11	59.01	8	72	11
16	12	1439	1	99.01	4	118.5	5
18	7	1279	6	29.41	12	102	7
17	10	1354	3	156.62	1	179	1

The result shows a very storng r_s between groundwater chloride and recharge. The result is expected since concentration of chloride in groundwater is inversely proportional to recharge. Moreover, chloride concentration in groundwater is strongly associated with aquifer resistivity obtained from VES curve (r_s = -0.76) (Table 4.6). The correlation indicates chloride in groundwater and recharge increase or decrease simultaneously. However, the relationship is inconclusive as resistivity of aquifer can be affected by other ions dissolved in water and aquifer material. The concentration of chloride and resistivity of groundwater is moderately correlated with groundwater resistivity (r_s = 0.43). The moderate correlation also indicates there are ionic concentration that affect the resistivity of pore water rather than chloride or pore fluid resistivity. In this case the conductivity might come from minerals.

Table 4.6 Spearman's rank correlation coefficient value for different parameters used.

	Cl_{gw} vs Recharge	**Cl_{gw} vs Groundwater resistivity**	**Cl_{gw} vs Aquifer resistivity**	**ρ_{gw} vs Aquifer resistivity**
r_s	-0.94	-0.43	-0.76	0.43
Description	Very strong	Moderate	Strong	Moderate

4.2 Groundwater Recharge Map of Thepkasattri

The point recharge estimated using the CMB method was interpolated to predict the spatial distribution of groundwater recharge. There are numerous geostatistical interpolators used to predict the unsampled value. Geostatistical interpolator IDW was applied using Arc Map.

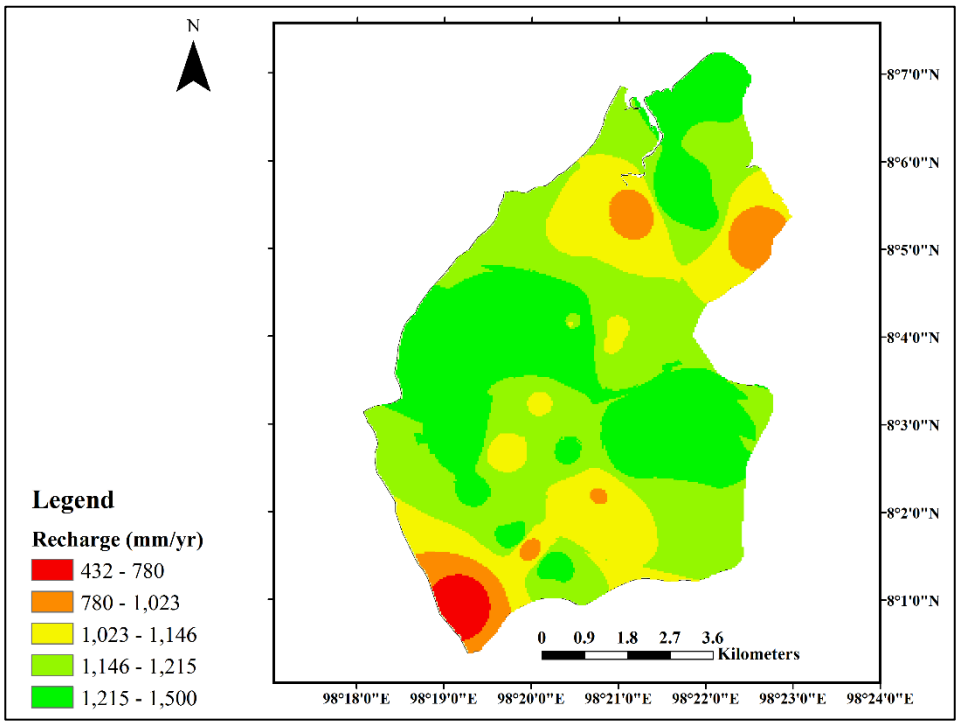

Figure 4.6 Showing groundwater recharge map of Thepkasattri.

The recharge map shows relatively low recharge value ranges from 432-780 mm/yr. in the south-west of the study area (Figure 4.6). This corresponds to land use and land cover of the study area (Figure 4.7). This region of the study area is highly populated settlements comprising residence house, commercial houses and shopping centers. Therefore, in this region urban runoff is more pronounced with minor infiltration. The highest recharge is in the eastern, western and northern catchment with amount ranges from 1215-1500 mm/yr. The land use land cover of the study area shows this region is covered by crops, forest, and mangrove. Based on Jayawickreme et al., (2008) study recharge is higher in land covered by crops than forest. This is due to higher evapotranspiration under forest than crops or grasslands. The median recharge values range from 780-1215 mm/yr. is found in the middle part of the study area. The central part is mainly covered by rubber plantation with minor scattered settlements.

The amount of recharge and spatial distribution in Thepkasattri is strongly dependent on the vertical hydraulic properties of the unsaturated zone, precipitation and land cover. The dependency of recharge is supported by water table fluctuation data, the land cover map, and time-lapse ERT.

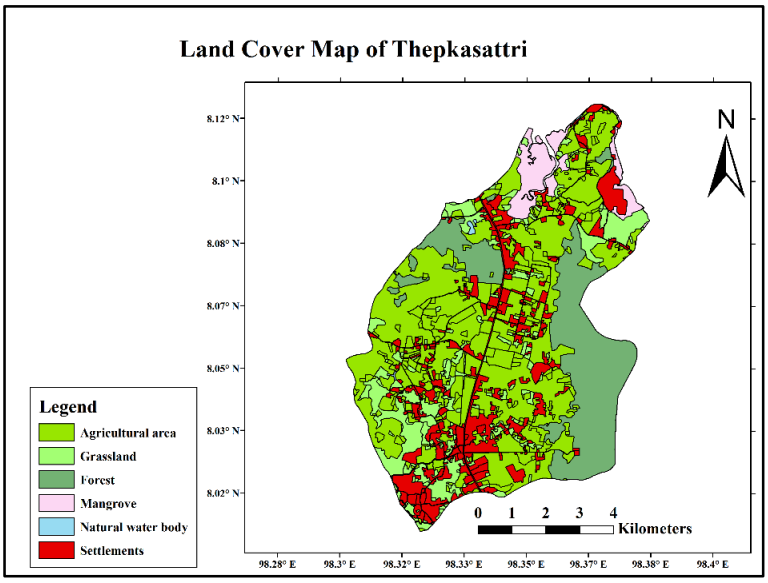

Figure 4.7 Showing 2016 land cover map of Thepkasattri sub-district modified after (Land Development Department, Thailand).

4.3 Seasonal Groundwater Recharge Characterization

4.3.1 Electrical Resistivity Data Analysis

Pre-interpretation analysis of data from electrical resistivity survey was done using EarthImager 2D. The pre-interpretation enhances interpretation ambiguity and ensures data quality. Therefore, the pre-interpretation has started by evaluating the contact resistance between the electrode and the ground. As the contact resistance test shows a majority of the electrodes has the recommended resistivity value of fewer than 2 KΩ. Then the relative model sensitivity was evaluated to observe the data quality from the top to the bottom of the profile as shown in Figure 4.8 and Figure 4.9.

The relative model sensitivity value for line one is decreasing to the bottom of the profile. This is due to the proximity of the electrodes to the shallow depth. However, on the three surveys done in line one, the March survey has relatively high model sensitivity with highest value 2.2 and the lowest is 0.000184 (Figure 4.8a). Hence the RMS error and L2 is lower for that survey data, 3.00% and 1.00 respectively. June survey has the lowest relative model sensitivity with maximum and minimum value 1.2 and 0.000041 respectively. Hence, higher misfit between measured and calculated

resistivity is evident (RMS = 3.67%, L2 = 1.50). This is evident by the number of iteration the software processed to fit the measured with calculated resistivity was eight (Figure 4.8b and Figure 4.9b).

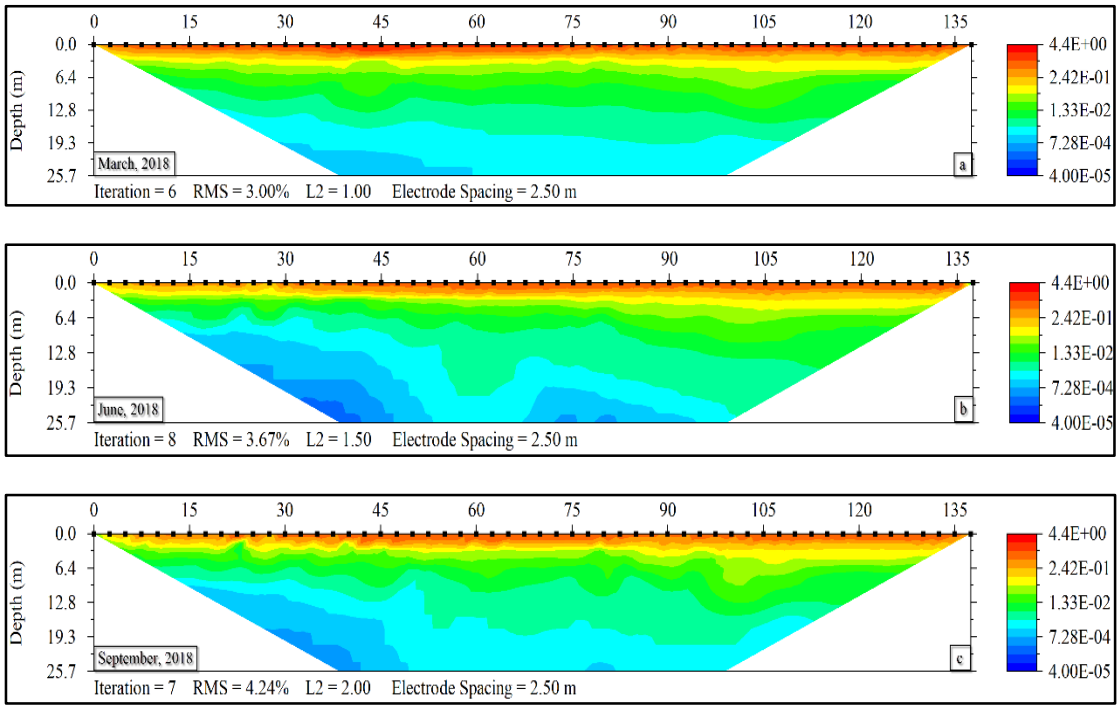

Figure 4.8 Relative model sensitivity for three ERT surveys in line one (a) March, (b) June, (c) September.

Crossplot of measured versus calculated resistivity data of ERT survey for line one in March, June and September is shown in Figure 4.9. The crossplot was done after the end of the inversion process. Generally, the data has a good fit between measured and calculated resistivity. The highest misfit is in September; this is expressed by the highest RMS error of 4.24%. However, this is not bad data since the RMS error is below the recommended value of 5.00%.

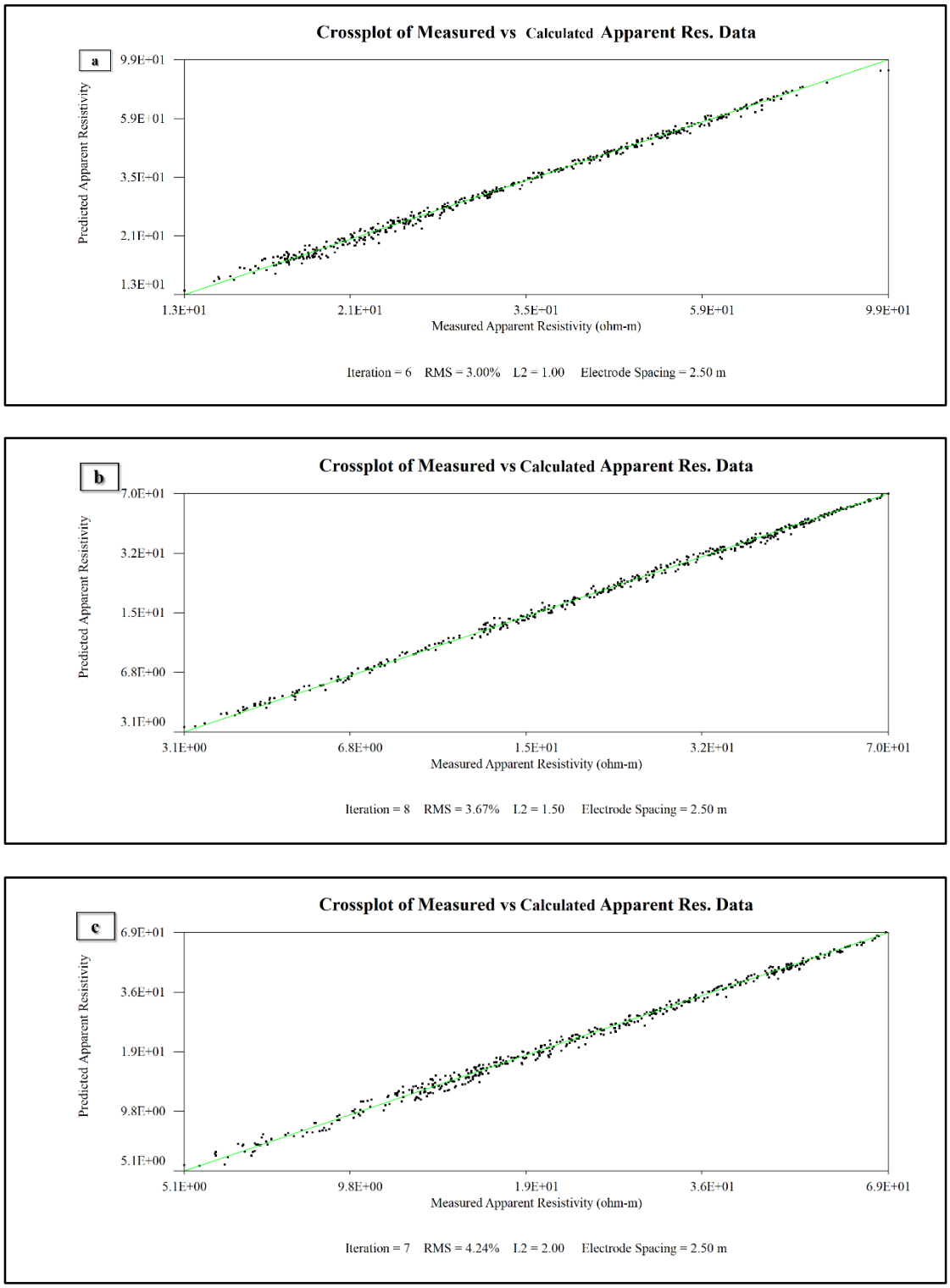

Figure 4.9 Showing line one crossplot of measured and calculated resistivity data: (a) March, (b) June, (c) September.

The relative model sensitivity for line two in March, June, and September is shown in Figure 4.10. Compared to line one this line has the highest model sensitivity. Hence the inversion was able to fit the measured apparent resistivity with calculated resistivity in not more than four iterations.

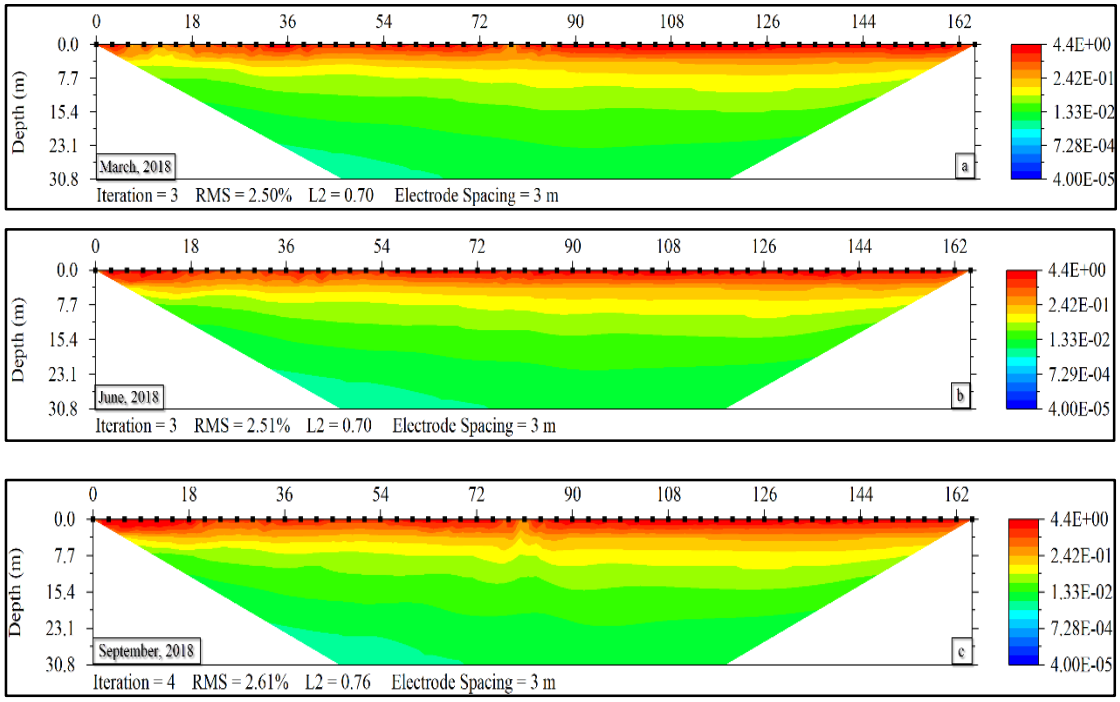

Figure 4.10 Relative model sensitivity for three ERT surveys in line two (a) March, (b) June, (c) September.

The crossplot of measured apparent resistivity for line two fitted well with the calculated resistivity at the lowest iteration 3 to 4. The majority of the data are projected in the green line with few outliers in June and September (Figure 4.11).

The relative model sensitivity indicates that the data collection was successful in measuring the resistivity value of the desired depth. In addition, the crossplot of predicted and calculated resistivity has RMS less than 5%; this implies the inversion model was suitable, and the data is worth for further interpretation and analysis.

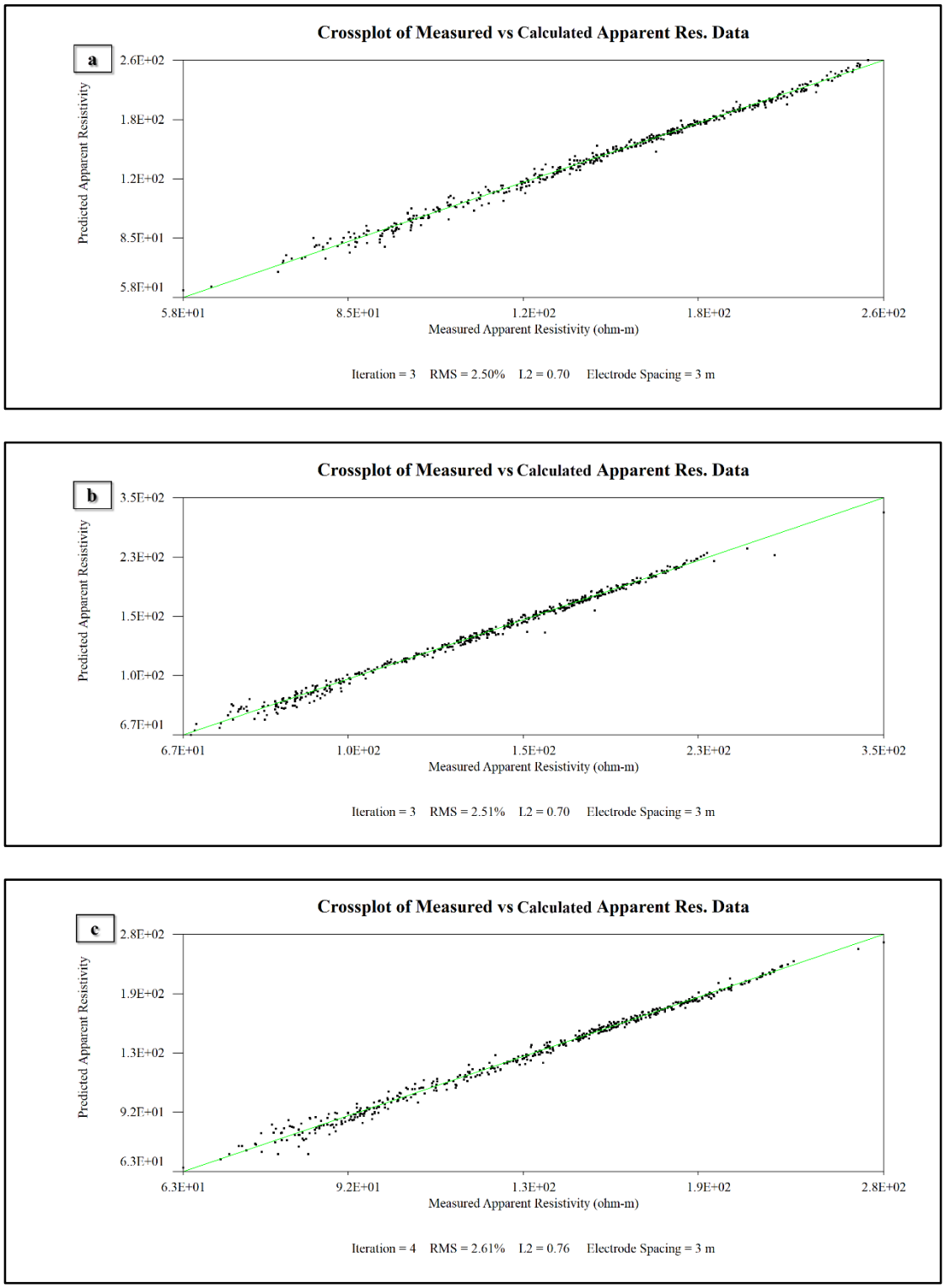

Figure 4.11 Showing line two crossplot of measured and calculated resistivity data: (a) March, (b) June, (c) September.

4.3.2 Well Log Data Preparation

Well, log data of the study area was obtained from DGR. The wells were drilled in a different time, and the geological section along with depth was recorded in their database. After a thorough evaluation of the data, two boreholes were selected for geological section preparation. The two boreholes were selected based on the proximity to ERT lines. The well log data shows there is a thick alluvial deposit in the flat plains underlained by weathered/fractured granite. While the topographic highs are represented by thin weathered/fractured granite underlained by granitic bedrock as shown in (Figure 4.12).

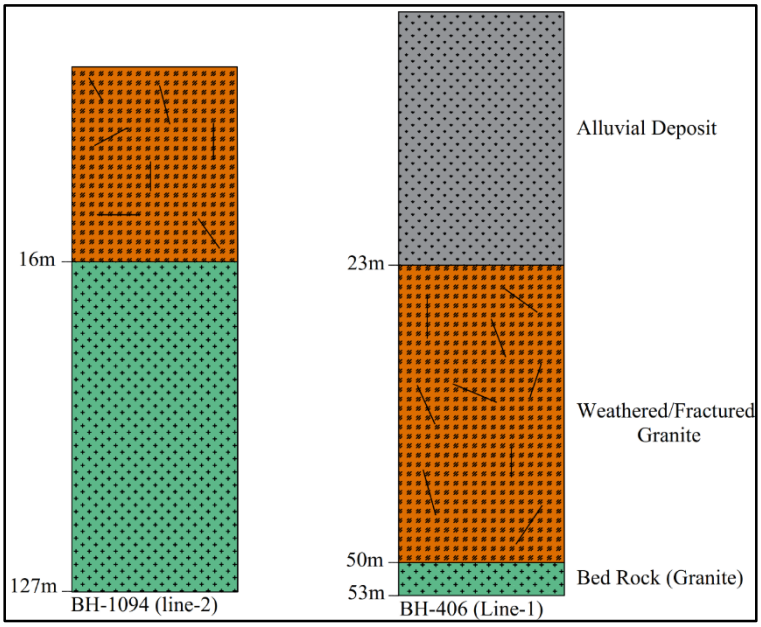

Figure 4.12 Well log data are showing the different stratigraphic section of the area under Line-1 and line-2.

4.3.3 Thepkasattri Line One ERT Interpretation

The water table fluctuation data is a measure of groundwater level in a monitoring well caused by recharge or discharge. Water level rise in piezometer responses to change in storage caused by water infiltration (recharge) (Healy and Cook 2002). On the other hand, the water level decline indicates discharge from the storage. Monitoring of water level fluctuation gives information on the dynamics of recharge on the local scale that represents a spatial area of thousands of square meters (Healy 2012). A piezometer installed by DGR was used to observe the water table fluctuation pattern.

Well hydrograph was plotted against average monthly precipitation for 2015 (Figure 4.13). The water table fluctuation trend follows the precipitation pattern of the study. The water level reaches the deepest level of 4.15m between March and April (dry season), then starts to rise during the wet season and reaches the peak (~1.65m) between July and September. The relationship between water level fluctuation and precipitation suggests the dependency of recharge on the climatic condition of the study area. This relationship further implies significant variations in resistivity of subsurface during the onset of wet season as anticipated.

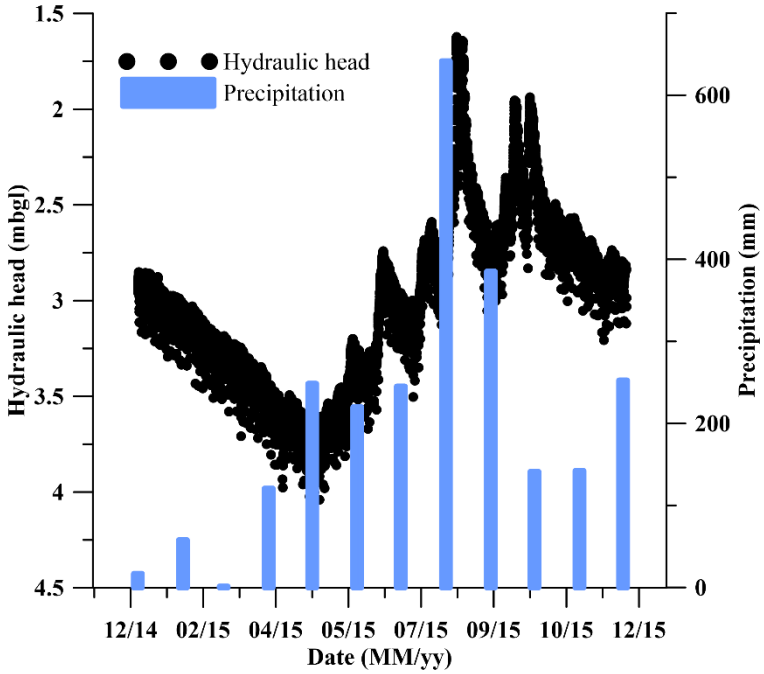

Figure 4.13 Well hydrograph is showing water table fluctuation versus precipitation.

The inverted electrical resistivity section of line one is shown in Figure 4.14. The first figure shows the dry season phenomena characterized by three horizons. The first horizon represented by blue colour has a resistivity value range from 4.8Ωm to 13Ωm (demarcated by black dot lines). This horizon is associated with water flux, and it doesn't extend up to the surface, but vertically extends from 3.2m to the bottom of the profile. There exists a low resistivity horizon at depth extending from the beginning of the profile to 52m distance (marked by horizontal black arrow). This layer is associated with water infiltration from the nearby stream located on the left side of the profile (Figure 3.1). In Figure 4.14b and Figure 4.14c the low resistivity horizon

extends up to the surface; this is due to superficial infiltration in response to rainfall from April to September. The effect of the stream water infiltration has pronounced at this time by a significant decrease in resistivity (demarcated by red dot lines). This implies more flux of water is coming from the stream and become part of the groundwater aquifer. However, the low resistivity horizon located between 45m and 75m distance in March profile disappeared in June and then re-emerged in September profile (Figure 4.14b marked by red crossed lines). The disappearance is associated with exterminated datasets during ERT inversion. Consequently, bad datum points were exterminated during ERT inversion. The bad datum points might be due to the high contact resistance between the electrode and ground. The number of iteration for this survey was eight resulting from the difficulty of fitting measured resistivity with calculated resistivity (Table 4.7 and Figure 4.9b).

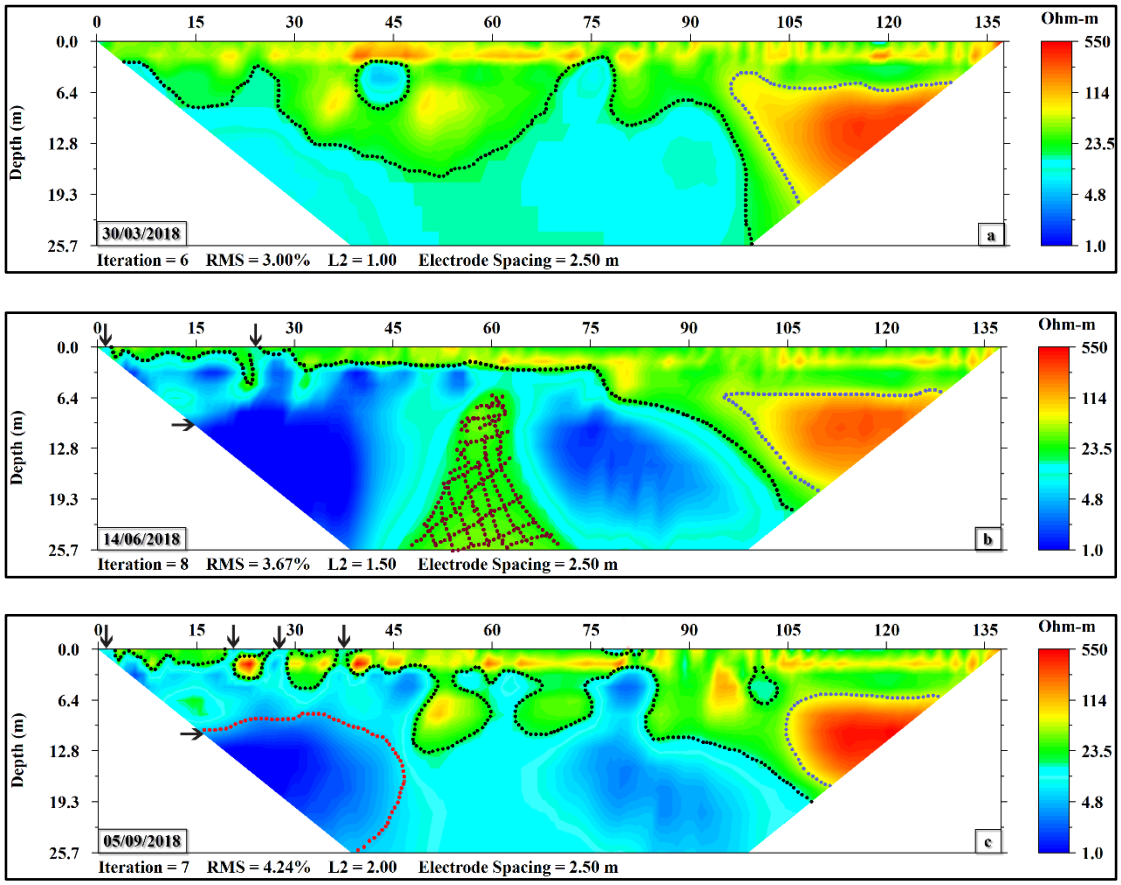

Figure 4.14 Electrical resistivity tomography of line one (a) March, (b) June, (c) September.

The second major horizon is represented by green and yellow colour with resistivity value ranges from 20 Ωm to 114 Ωm. This layer is associated with alluvial deposit consist of sandy clay and gravely sand.

The third horizon is the most resistive layer located at distance 97m to the end of profile and vertically from 6.2m to 19.3m and at the top part of each profile (Figure 4.14a, Figure 4.14b, Figure 4.14c). The resistivity value of this layer ranges from 115 Ωm to 550 Ωm (demarcated by a blue dot line). The resistive body located at 105m distance onwards might be a 3D artifact associated with minor elevation change (Arora and Ahmed 2011) or it might be due to dry or impermeable rock. The top part of the resistive horizon has undulating shape due to preferential water flow paths.

4.3.4 Thepkasattri Line Two ERT Interpretation

A piezometer coupled with rain gauge installed in May 2018 at CDPM station was used to observe water table fluctuation during the ERT survey time. The piezometer records water level and precipitation on an hourly basis throughout the day. The well hydrograph along with a variation of rainfall in the study area is shown in Figure 4.15. It is clear that there is a positive linear correlation between water level rise and the amount of precipitation. Water level starts to rise in May, corresponding to the onset of the rainy season. The water level reaches a peak value of 3.6m (bgl) at the end of the rainy season. The peak water level corresponds to the highest precipitation of 56mm. This correlation further indicates that recharge is episodic and dependent on the amount of precipitation and the hydraulic property of the vadose zone.

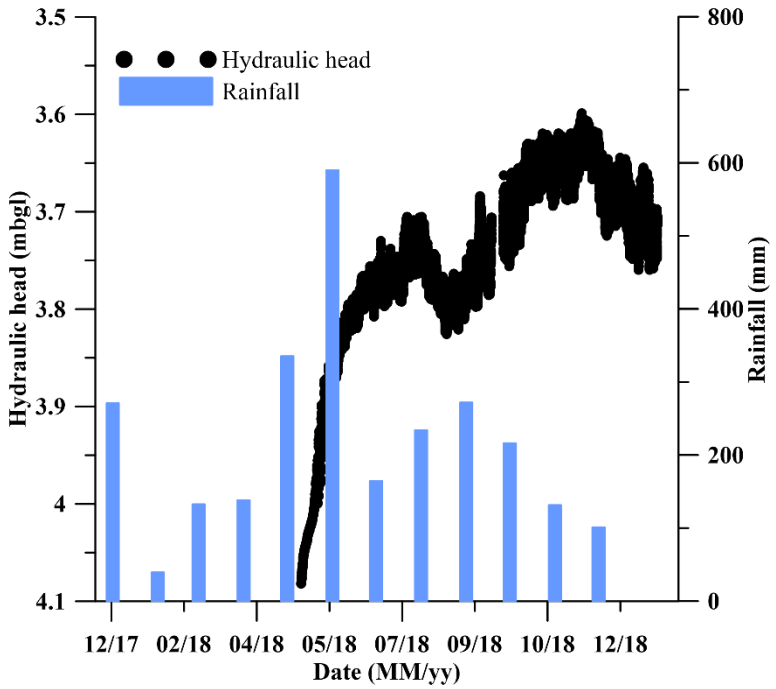

Figure 4.15 Well hydrograph is showing water table fluctuation versus daily precipitation.

The inversion result of line two shows, the tomography is dominated by two horizons with colour representation orange/green and red as shown in Figure 4.16a. The low resistivity layer is represented by orange colour and irregularly distributed green colour. The resistivity value of the layer (demarcated by black dot lines) ranges from 14Ωm to 100Ωm. The layer extends to a 23.1m depth at a 36m distance and further from that location the layer pinches out. At 139m to 157m distance, the layer found only to 7.7m depth in all profiles. This layer is associated with water saturated weathered and fractured granite. However, the shape of the layer slightly increased vertically in June and September profile and this change is attributed due to surficial infiltration during the wet season.

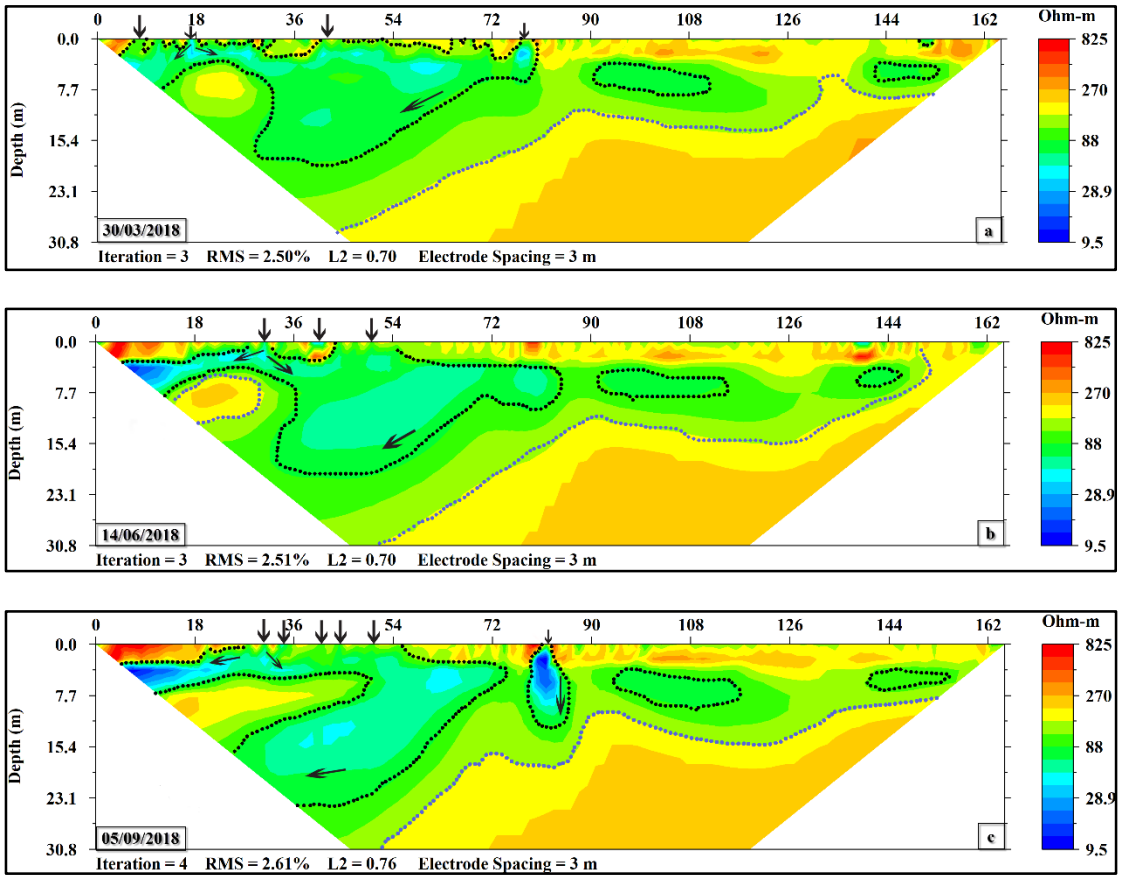

Figure 4.16 Electrical resistivity tomography of line two (a) March, (b) June, (c) September.

The most conductive blue/light blue horizon is represented by the resistivity value of 13Ωm to 68Ωm shows a variation of shape throughout the three dates (marked by black arrows). The variation is prominent between the dates of March and June. While the September profile shows a slight size increase compared to June profile. The overall variation of the horizon indicates the movement of water flux. At an 81m distance, the horizon (marked by red arrow) extends from 3m in March to around 12m in September. This implies a vertical water movement in the vadose zone.

Similarly, the horizon shows variation between 4.5m to 68m distance, indicating water flux movement both vertically and horizontally. Beside that from the beginning of the profile to 81m distance, the blue/green horizon shows size enlargement towards the beginning of the profile to 20m depth in September tomography. In this profile, there is resistivity value change characterized by crescent shape, associated with preferential flow from the vadose zone located at an 18m distance (marked by

horizontal black arrows). The resistivity change in all three profiles implies interflow and groundwater flow to the stream located on the left part of the profile.

Table 4.7 Electrical resistivity inversion statistics.

Date	Array	Iterations		RMS (%)	
		Line-1	Line-2	Line-1	Line-2
March	Wenner	6	3	3.00	2.50
June	Wenner	8	3	3.67	2.51
September	Wenner	7	4	3.20	2.61

The second dominant horizon is the most resistive layer represented by yellow/reddish colour with a resistivity value range from 300Ωm to 550Ωm (demarcated by blue dot lines). This layer comprises most of the left side of the profile. The horizon regularly extends from 40m to 165m distance. Based on the well log data the layer corresponds to granite bedrock (Figure 4.12).

Water level fluctuation along with the variation of rainfall in the study area is shown in Figure 4.15. It is clear that the water level rise is a direct response to the amount of precipitation. The rainy season starts in May and continues until the beginning of October. Similarly, the water level starts to rise in May, though there is no measurement record between February and March. However, the overall trend shows water level falls during the absence or few precipitations. Then the water level reaches a peak at the end of the wet season. The peak water level corresponds to the highest precipitation of 56mm Figure 4.15.

Similarly, for the year 2015 water table fluctuation data, the water table falls during the dry season and starts to rise with the beginning of the rainy season. This relationship of water level fluctuation with precipitation further indicates that recharge is episodic that depend on the amount of precipitation. In addition, significant variations in resistivity of the subsurface are anticipated.

Table 4.8 Stream water electrical conductivity variation in both locations.

Month	Stream water EC (µS/cm)	
	Line-1	**Line-2**
June	120.1	70.1
September	101.4	72.9
σ	**13.22**	**1.98**

The EC of stream water measured in June and September are presented in Table 4.8. The table shows low EC of the stream in site nearby line one than in line two. This indirectly indicates the resistivity of pore water in the location one and two. Hence, the resistivity of the conductive layer in line one is much lower than line two.

4.3.5 Time-Lapse ERT Interpretation

Time-lapse inversion was done using EarthImager 2D 2.4.4 after following the standard procedure given in the manual (Advanced Geosciences Inc. 2014). The least square inversion model was used for all time-lapse ERT data sets. The time-lapse ERT data was inverted by setting the dry season profile as a base model for the following June and September profiles. Then the data was presented as the difference in resistivity in the scale of 100% to -100%.

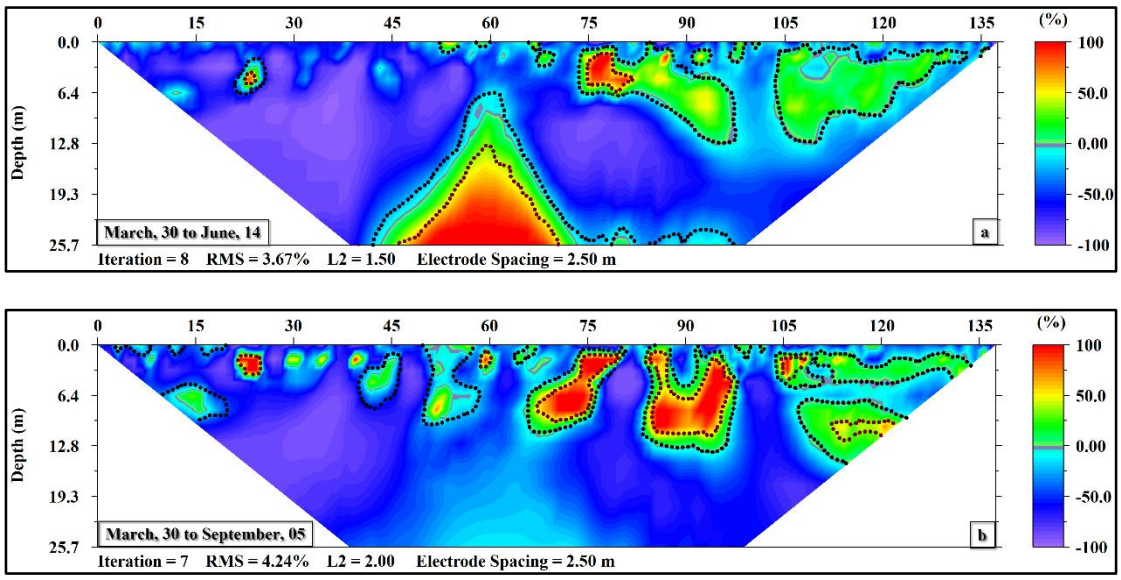

Figure 4.17 Time-lapse ERT inversion of line one with respect to March profile (a) March to June (b) March to September.

Time-lapse ERT inversion of line one from March to June and March to September is shown in Figure 4.17a and Figure 4.17b. On the right side of both profiles starting from the initial distance to the distance 135m, there is strong resistivity decrease ranging from -50% to -100% (demarcated by black dot lines). This strong resistivity change extends from the surface to the bottom of the profile. This implies infiltration from the surface and the stream (marked by black arrow). The strong resistivity decrease indirectly indicates peak water saturation of the layer. The preferential recharge zones are regularly connected with the bottom aquifer between 0 and 135m distance creating funneled flow. However, in (Figure **4.17**b) the preferential flow occurs as patches on the top of the layer to 9.6m depth. This irregularity is associated with the relocation of electrodes and bad datum points. There are irregularly distributed areas characterized by green colour and represented by 0 to 50% resistivity increase associated with heterogeneity within the layer and instrument error. The resistive layer represented by yellow to red colour shows a strong resistivity increase from 50% to 100%.

In Figure 4.17a the resistive body located horizontally starting from 48m to 72m and vertically from 12.8m to the bottom of the profile. This layer later disappeared in March-September time-lapse inversion (Figure **4.17**b). This clearly indicates the resistive layer is caused due to the bad datum in June profile. In addition, in (Figure 4.17a) an increase in resistivity is shown at 75m to 85m distance and 1m to 6.4m depth. Similarly, in Figure 4.17b irregularly distributed patches of an increase in resistivity are found from 22m to 97m distance and between 1.5m to 9.6m depth (Figure **4.17**b). The anomaly is associated with time-lapse inversion artifact. In both time-lapse inversions, there is a decrease resistivity value below the water table. The decrease in resistivity might occur because of two reasons. The first reason can be due to ionic concentration of groundwater at depth (Clément et al. 2009b). The second reason can be due to low ERT model resolution at depth, or it might be due to the effect of the overlying conductive layer (Loke 2000; Pellicer et al. 2012).

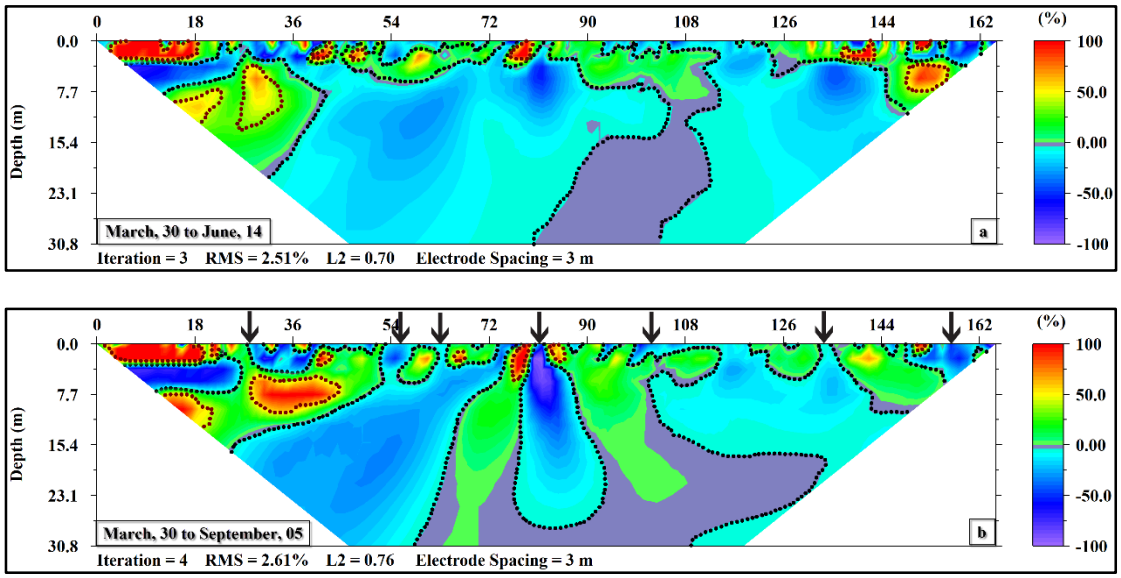

Figure 4.18 Time-lapse ERT inversion of line one with respect to March profile (a) March to June, (b) March to September.

Time-lapse ERT inversion of line two date March to June and March to September is shown in Figure 4.18a and Figure 4.18b. This profile is dominated by less than 50% resistivity decrease (demarcated by black dot lines). This strong resistivity change is associated with the first rainfall occurred during the months from April to September. In Figure 4.18a the resistivity decrease is attributed through preferential recharge zones located between 27m and 122m. This implies water infiltrated through these preferential zones are recharging the aquifer below. Similar preferential recharge zone is observed from March to September time-lapse inversion as well. In Figure 4.18a profiles the top part of the tomography is characterized by unstable flow concentrated into conductive fingers. In March to September time-lapse profile, some of the conductive fingers become preferential recharge zones (X = 27m, 54m, 63m, 104m, 135m, 157m) demarcated by vertical black arrows. The complicated preferential flow in vadose is associated with textural heterogeneity and hydraulic properties of the weathered/fractured granite (Nimmo 2009).

There exists a layer represented by resistivity increase from 5% to 50%. This layer mainly occurs in a top part of the profile and at the left side of the profile from 9m to 40m distance and vertically from 3m to 21m. This layer might be associated with low permeability body that is part of the granite bedrock. Then later in March to

September time-lapse ERT, the size seems to decrease vertically by 4m. Alongside there is a resistive body characterized by 70% to 100% resistivity increase. The resistive layer extends from surface to 11m depth. The resistive layer is inversion artifact produced by with fitting difficulty due to large resistivity variation. The inversion artifact is attributed by a change in moisture content or relocation of electrodes during those dates (Carey et al. 2017; Miller et al. 2008; Mojica et al. 2013).

In this area average groundwater level is 4.0m, which is 1.0m below or above the stream bed depending on the season. This implies groundwater is discharging as a base flow through the stream. This assumption is supported by time-lapse ERT, where the recharge through the first preferential recharge zone (X = 27m) is flowing toward the stream and there is no any infiltration coming from the stream in all dates.

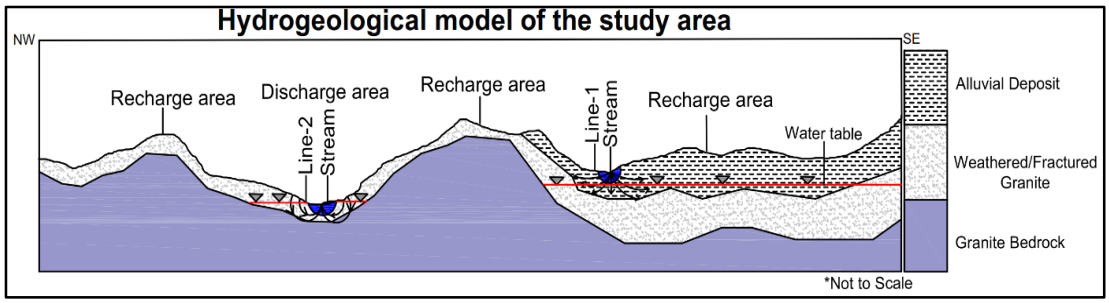

Figure 4.19 A simplified hydrogeological model of the study area.

The resistivity variation between dry season and wet season is much higher in line one than line two. This is expressed by approximately 100% resistivity decrease in line one, while in line two is 75% decrease. This shows the effect of the stream in line one and also the hydrogeology of the vadose zone. Geologically the vadose zone in line one is an alluvial deposit and in line two is weathered/fractured granite (Figure 4.12). This implies in weathered/fractured granite recharge is controlled by slow flow pathways as shown in three tomograms in Figure 4.16 and Figure 4.17. Considering the time-lapse ERT and groundwater data of the study area a simplified hydrogeological model of the study area is presented in Figure 4.19.

CHAPTER 5

CONCLUSIONS

Groundwater recharge estimation in Thepkasattri was evaluated using the CMB and the WTF method. The mean recharge estimated using the CMB method is 1172mm/yr. These represent 47% of the annual rainfall in Thepkasattri. In another hand, mean recharge estimated using the WTF method is 19% for monitoring well located in the study area. Based on the concentration factor, a concentration factor of 0.47 indicates 53% annual rainfall loss through evapotranspiration.

Moreover, recharge in Thepkasattri is episodic that depend on the amount of precipitation and vertical hydraulic conductivity of the unsaturated zone. This assumption is further supported by time-lapse ERT in two locations. In addition, the spatial distribution of recharge in Thepkasattri is strongly influenced by land cover and land use of the area. The land covered by agriculture and forest recorded higher recharge than the land covered by settlements. Further research on urban planning and water resources management issue is warranted.

In addition, time-lapse electrical resistivity was applied to investigate seasonal groundwater recharge variation in Thepkasattri watershed. Time-lapse electrical resistivity survey is a non-destructive method and provides a spatial and temporal variation of water infiltration in the vadose zone. Well, log data was used to identify the geology of the subsurface. The integration of hydrogeological and geophysical data in the study area was useful for reducing the uncertainty of ERT interpretation. The variation in groundwater recharge (moisture content) is expressed as the percentage difference of resistivity between the base profile and monitoring profiles.

In line one and line two strong resistivity variation was observed in the vadose zone during the wet season. The maximum resistivity decrease in line one reaches around 100 %, while in line two it is around 75%. The decrease in resistivity is related to infiltrations produced by rainfall during the rainy season. The stream draining near line one was identified as the recharge zone. While the stream draining in line two is a gaining stream and identified as a discharge zone. The interpretation was further supported by groundwater data of the area and field observation. Based on the two electrical resistivity results and the well hydrograph the aquifer replenishment is mainly done by water infiltration through the vadose zone. This study shows the applicability of time-lapse ERT method on visualizing the spatiotemporal degree of saturation and identifying preferential recharge zones.

REFERENCES

Advanced Geosciences Inc. (2014). *Instruction Manual for EarthImager 2D Version 2.4.0. Resistivity and IP Inversion Software*.

Afrifa, G. Y., Sakyi, P. A., and Chegbeleh, L. P. (2017). "Estimation of groundwater recharge in sedimentary rock aquifer systems in the Oti basin of Gushiegu District, Northern Ghana". *Journal of African Earth Sciences*, Elsevier Ltd, 131, 272–283.

Aishlin, P. S. (2006). "Groundwater recharge estimation using chloride mass balance dry creek experimental watershed". Boise State University.

Arora, T., and Ahmed, S. (2011). "Characterization of recharge through complex vadose zone of a granitic aquifer by time-lapse electrical resistivity tomography". *Journal of Applied Geophysics*, Elsevier B.V., 73(1), 35–44.

Berthold, S., Bentley, L. R., and Hayashi, M. (2004). "Integrated hydrogeological and geophysical study of depression- focused groundwater recharge in the Canadian prairies". *Water Resources Research*, 40, 1–14.

Blarasin, M., Maldonado, L., Quinodoz, F., Cabrera, A., Matteoda, E., Alincastro, N., and Albo, G. (2016). "Weekly and Monthly Groundwater Recharge Estimation in A Rural Piedmont Environment using the Water Table Fluctuation Method". *International Journal of Environmental & Agriculture Research*, 2(May), 104–113.

Carey, A. M., Paige, G. B., Carr, B. J., and Dogan, M. (2017). "Forward modeling to investigate inversion artifacts resulting from time-lapse electrical resistivity tomography during rainfall simulations". *Journal of Applied Geophysics*, Elsevier B.V., 145(August), 39–49.

Charoenpong, S., Suwanprasit, C., and Thongchumnum, P. (2012). "Impacts of interpolation techniques on groundwater potential modeling using GIS in Phuket Province, Thailand". *33rd Asian Conference on Remote Sensing 2012, ACRS 2012*, 732–738.

Charusiri, P., Pongsapich, W., and Vedchakanchana, S. (1986). "Petrological and Geochemical studies of granites of Kathu Plutons of Phuket Island, Southern

Thailand". *Bulletin of the Geological Society of Malaysia*, 261–280.

Clément, R., Descloîtres, M., Gunther, T., and Oxarango, L. (2009a). "Comparison of three arrays in time-lapse ERT: Simulation of a leachate injection experiment". *ArchéoSciences*, 33(33 (suppl.)), 275–278.

Clément, R., Descloitres, M., Günther, T., Ribolzi, O., and Legchenko, A. (2009b). "Influence of shallow infiltration on time-lapse ERT: Experience of advanced interpretation". *Comptes Rendus - Geoscience*, 341(10–11), 886–898.

Covitt, B. A., Hinojosa, T. T., Marcos-Iga, J., Matz, M. S., Miller-Rushing, A., Miller-Rushing, A., Posner, A. J., and Treiber, T. G. (2012). "Earth's freshwater, A guide for teaching freshwater in grades 3 to 8". *Environmental literacy techer guide series*.

Delin, G. N., Healy, R. W., Lorenz, D. L., and Nimmo, J. R. (2007). "Comparison of local- to regional-scale estimates of ground-water recharge in Minnesota, USA". *Journal of Hydrology*, 334(1–2), 231–249.

Descloitres, M., Ruiz, L., Sekhar, M., Legchenko, A., Braun, J., Kumar, M. S. M., and Subramanian, S. (2008). "Characterization of seasonal local recharge using electrical resistivity tomography and magnetic resonance sounding". *Hydrological Processes*, 22(May 2007), 384–394.

Grynkiewicz, M., Polkowska, Z., Zygmunt, B., and Namieśnik, J. (2003). "Atmospheric precipitation sampling for analysis". *Polish Journal of Environmental Studies*, 12(2), 133–140.

Hagedorn, B., El-Kadi, A. I., Mair, A., Whittier, R. B., and Ha, K. (2011). "Estimating recharge in fractured aquifers of a temperate humid to semiarid volcanic island (Jeju, Korea) from water table fluctuations, and Cl, CFC-12 and 3H chemistry". *Journal of Hydrology*, Elsevier B.V., 409(3–4), 650–662.

Healy, R. (2012). *Estimating Groundwater Recharge*. *Cambridge University Press*, Published in the United Kingdom by Cambridge University Press, United Kingdom.

Healy, R. W., and Cook, P. G. (2002). "Using groundwater levels to estimate recharge".

Hydrogeology Journal, 10(1), 91–109.

Hummel, C. L., and Phawandon, P. (1967). *Geology and Mineral Deposits of the Phuket Mining District, South Thailand*.

Israil, M., Al-hadithi, M., Singhal, D., and Kumar, B. (2006). "Groundwater-recharge estimation using a surface electrical resistivity method in the Himalayan foothill region , India". *Hydrogeology Journal*, 14, 44–50.

Jayawickreme, D. H., van Dam, R. L., and Hyndman, D. W. (2008). "Subsurface imaging of vegetation, climate, and root-zone moisture interactions". *Geophysical Research Letters*, 35(18), 1–5.

Johnson, a. I. (1963a). "Specific Yield - Compilation of Specific Yields for Various Materials". *USGS Open-File Report*, (63–59), 119.

Johnson, A. I. (1963b). *Compilation of Specific Yield for Various Materials*.

Kearey, P., Brooks, M., and Hill, I. (2002). *An Introduction to Geophysical Exploration*. Blackwell Science.

Kong, S. O. (2017). "Hydrogeological Characterization of Phuket Aquifer System with Reference to Groundwater Development of Phuket, Thailand". Prince Songkla University, Phuket Campus.

Lin, J., Cai, G., Liu, S., Puppala, A. J., and Zou, H. (2017). "Correlations Between Electrical Resistivity and Geotechnical Parameters for Jiangsu Marine Clay Using Spearman's Coefficient Test". *International Journal of Civil Engineering*, Springer International Publishing, 15(3), 419–429.

Loke, M. H. (2000). *Electrical imaging surveys for environmental and engineering studies*.

Loke, M. H., Acworth, I., and Dahlin, T. (2003). "A comparison of smooth and blocky inversion methods in 2D electrical imaging surveys". *Exploration Geophysics*, 34(3), 182–187.

M-BRACE. (2014). *URBAN VULNERABILITY IN SOUTHEAST ASIA Summary of Vulnerability Assessments in Mekong-Building Climate Resilience in Asian Cities (M-BRACE) URBAN VULNERABILITY IN SOUTHEAST ASIA Summary of*

Vulnerability Assessments in Mekong-Building Climate Resilience.

Machiwal, D., Singh, P. K., and Yadav, K. K. (2016). "Estimating aquifer properties and distributed groundwater recharge in a hard-rock catchment of Udaipur, India". *Applied Water Science*, Springer Berlin Heidelberg, 7(6), 3157–3172.

Mensah, O., Alo, C., and Yidana, S. M. (2014). "Evaluation of groundwater recharge estimates in a partially metamorphosed sedimentary basin in a tropical environment: application of natural tracers". *TheScientificWorldJournal*, 2014(10.1155), 419508.

Miller, C. R., Routh, P. S., Brosten, T. R., and McNamara, J. P. (2008). "Application of time-lapse ERT imaging to watershed characterization". *Geophysics*, 73(3), G7.

Ministry of Agriculture and Cooperatives. (2011). *Reference Crop Evapotranspiration Penman Monteith*.

Mojica, A., Díaz, I., Ho, C. A., Ogden, F., Pinzón, R., Fábrega, J., Vega, D., and Hendrickx, J. (2013). "Study of seasonal rainfall infiltration via time-lapse surface electrical resistivity tomography: Case study of Gamboa area, Panama Canal Watershed". *Air, Soil and Water Research*, 6(December 2013), 131–139.

Nimmo, J. R. (2009). "Vadose Water". *Encyclopedia of Inland Waters*, 1, 766–777.

Pellicer, X. M., Zarroca, M., and Gibson, P. (2012). "Time-lapse resistivity analysis of Quaternary sediments in the Midlands of Ireland". *Journal of Applied Geophysics*, Elsevier B.V., 82, 46–58.

Ritorto, M. (2007). "Imapacts of diffuse recharge on transmissivity and water budget". University of Florida.

Saghravani, S. R., Yusoff, I., Wan Md Tahir, W. Z., and Othman, Z. (2014). "Comparison of water table fluctuation and chloride mass balance methods for recharge estimation in a tropical rainforest climate: a case study from Kelantan River catchment, Malaysia". *Environmental Earth Sciences*, 73(8), 4419–4428.

Saghravani, S. R., Yusoff, I., Wan Md Tahir, W. Z., and Othman, Z. (2015). "Estimating recharge based on long-term groundwater table fluctuation monitoring in a shallow aquifer of Malaysian tropical rainforest catchment".

Environmental Earth Sciences, Springer Berlin Heidelberg, 74(6), 4577–4587.

Samouëlian, A., Cousin, I., Tabbagh, A., Bruand, A., and Richard, G. (2005). "Electrical resistivity survey in soil science : a review". *Soil and Tillage Research*, 83, 173–193.

Scanlon, B. R., Healy, R. W., and Cook, P. G. (2002). "Choosing appropriate technique for quantifying groundwater recharge". *Hydrogeology Journal*, 10, 18–39.

Skinner, B., and Murck, B. (2011). *The Blue Planet an Introduction to Earth System Science*. Library of Congress Cataloging-in-Publication Data.

Somaratne, N., and Smettem, K. R. J. (2014). "Theory of the generalized chloride mass balance method for recharge estimation in groundwater basins characterised by point and diffuse recharge". *Hydrology and Earth System Sciences Discussions*, 11(1), 307–332.

Takounjou, A. F., Ngoupayou, J. R. N., Riotte, J., Takem, G. E., Mafany, G., Maréchal, J. C., and Ekodeck, G. E. (2011). "Estimation of groundwater recharge of shallow aquifer on humid environment in Yaounde, Cameroon using hybrid water-fluctuation and hydrochemistry methods". *Environmental Earth Sciences*, 64(1), 107–118.

Thai Industrial Standards Institute (TISI). (n.d.). "List of Accredited Laboratories According to ISO/IEC 17025". <https://appdb.tisi.go.th/tis_devs/tislab/lab_test2e.php?data=active&offsetA=3&offsetB=16> (May 20, 2019).

"Thalang District - Wikipedia". (2018). <https://en.wikipedia.org/wiki/Thalang_District> (Apr. 10, 2018).

Tirado, R., Englande, A. J., Promakasikorn, L., and Novotny, V. (2008). *Use of Agrochemicals in Thailand and its Consequences for the Environment*. *Greenpeace Research Laboratories Technical Note 03/2008*.

U.S. Geological Survey. (2015). *National Field Manual for the Collection of Water-Quality Data*. *Techniques of Water-Resources Investigations*.

Varni, M., Comas, R., Weinzettel, P., and Dietrich, S. (2013). "Application of the water

table fluctuation method to characterize groundwater recharge in the Pampa plain, Argentina". *Hydrological Sciences Journal*, Taylor & Francis, 58(7), 1445–1455.

Williams, M. (2014). "What Percent Of Earth is Water?" *23 April*, (2, December), 1.

Wood, W. W. (1999). "Use and Misuse of the Chloride-Mass Balance Method in Estimating Ground Water Recharge". *Ground Water*, 37(1), 2–3.

Wood, W. W., and Sanford, W. E. (1995). "Chemical and isotopic methods for quantifying ground-water recharge in a regional, semiarid environment". *Ground Water*, 33(3), 458+.

Yidana, S. M., and Koffie, E. (2014). "The groundwater recharge regime of some slightly metamorphosed neoproterozoic sedimentary rocks: An application of natural environmental tracers". *Hydrological Processes*, 28(7), 3104–3117.

APPENDICES I

Appendices I: Groundwater sampling wells location (Latitude and Longitude), annual recharge and evapotranspiration.

Well-ID	Latitude	Longitude	Well Depth (m)	Recharge (mm/yr.)	% Annual Rainfall	ET_f (mm/yr.)
GW02	8.026308	98.33309	68	853	34	1622.50
GW03	8.022923	98.33705	65	1439	58	1036.41
GW04	8.032271	98.32906	60	1211	49	1263.55
GW06	8.033481	98.34441	74	1151	47	1324.13
GW07	8.036098	98.34607	65	1001	40	1474.24
GW08	8.033346	98.34477	121	1046	42	1428.75
GW09	8.037254	98.32259	78	1279	52	1196.25
GW10	8.016366	98.32057	24	443	18	2032.36
GW11	8.085854	98.34070	42	1151	47	1324.13
GW12	8.069040	98.34083	27	1151	47	1324.13
GW15	8.110394	98.36408	120	1354	55	1121.03
GW16	8.105468	98.36596	70	1211	49	1263.55
GW17	8.044509	98.34030	50	1279	52	1196.25
GW18	8.048315	98.36145	45	1354	55	1121.03
GW19	8.046369	98.32151	22	1354	55	1121.03
GW20	8.070340	98.33348	40	1279	52	1196.25
GW21	8.044507	98.32740	60	1096	44	1378.93
GW22	8.065100	98.34835	121	1151	47	1324.13
GW24	8.065698	98.34341	36	1279	52	1196.25
GW25	8.068457	98.34932	33	1151	47	1324.13
GW27	8.090198	98.35331	120	853	34	1622.50
GW28	8.089369	98.36692	61	1279	52	1196.25
GW29	8.054034	98.33496	105	1151	47	1324.13
GW30	8.044094	98.35209	54	1354	55	1121.03
GW31	8.086333	98.37472	74	885	36	1589.71
GW32	8.093592	98.36051	61	1439	58	1036.41
GW33	8.117200	98.20214	28	1211	49	1263.55
GW34	8.172500	98.19812	105	1439	58	1036.41

APPENDICES II

Appendices II: Resistivity versus depth plot measured from vertical electrical sounding.

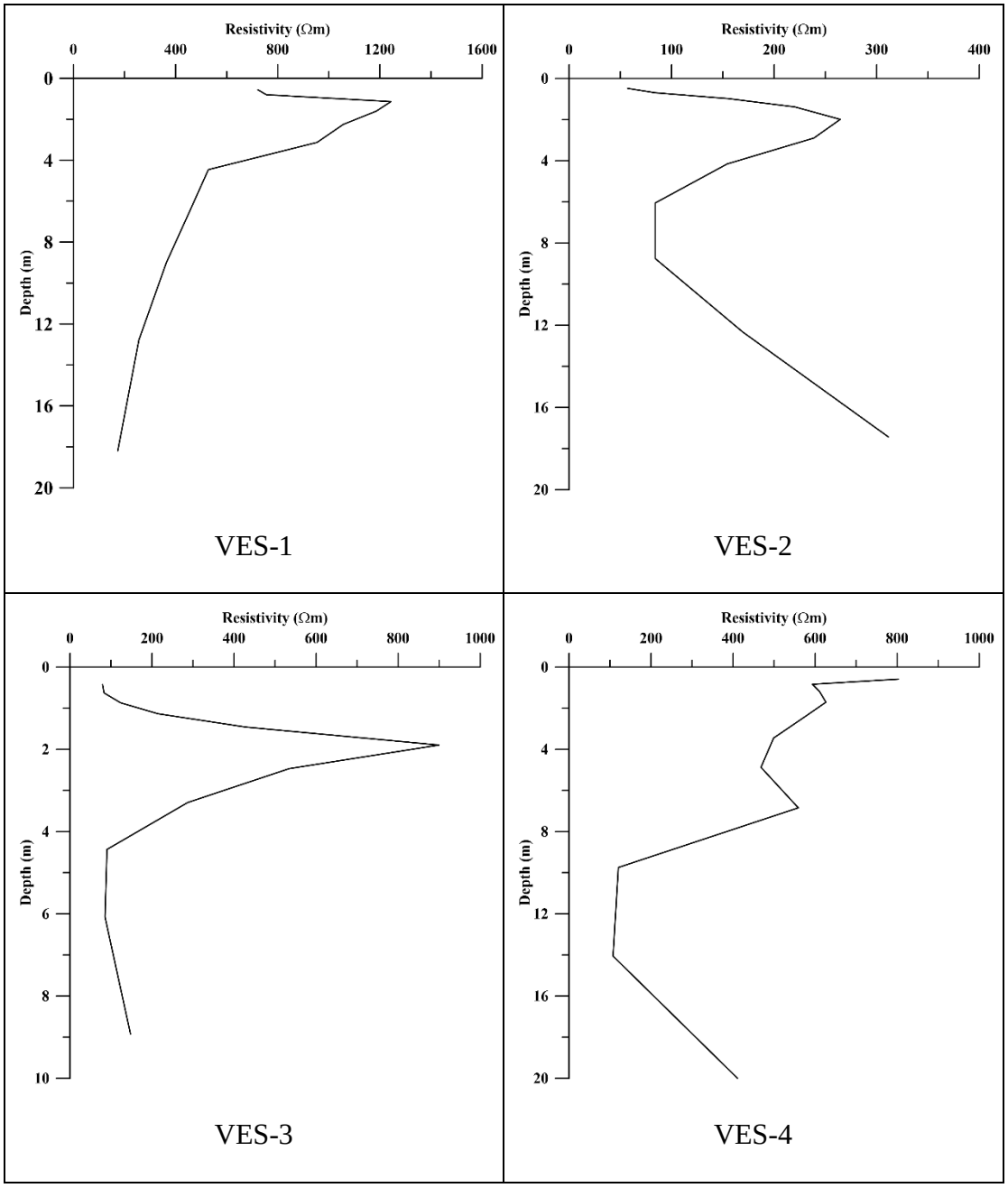

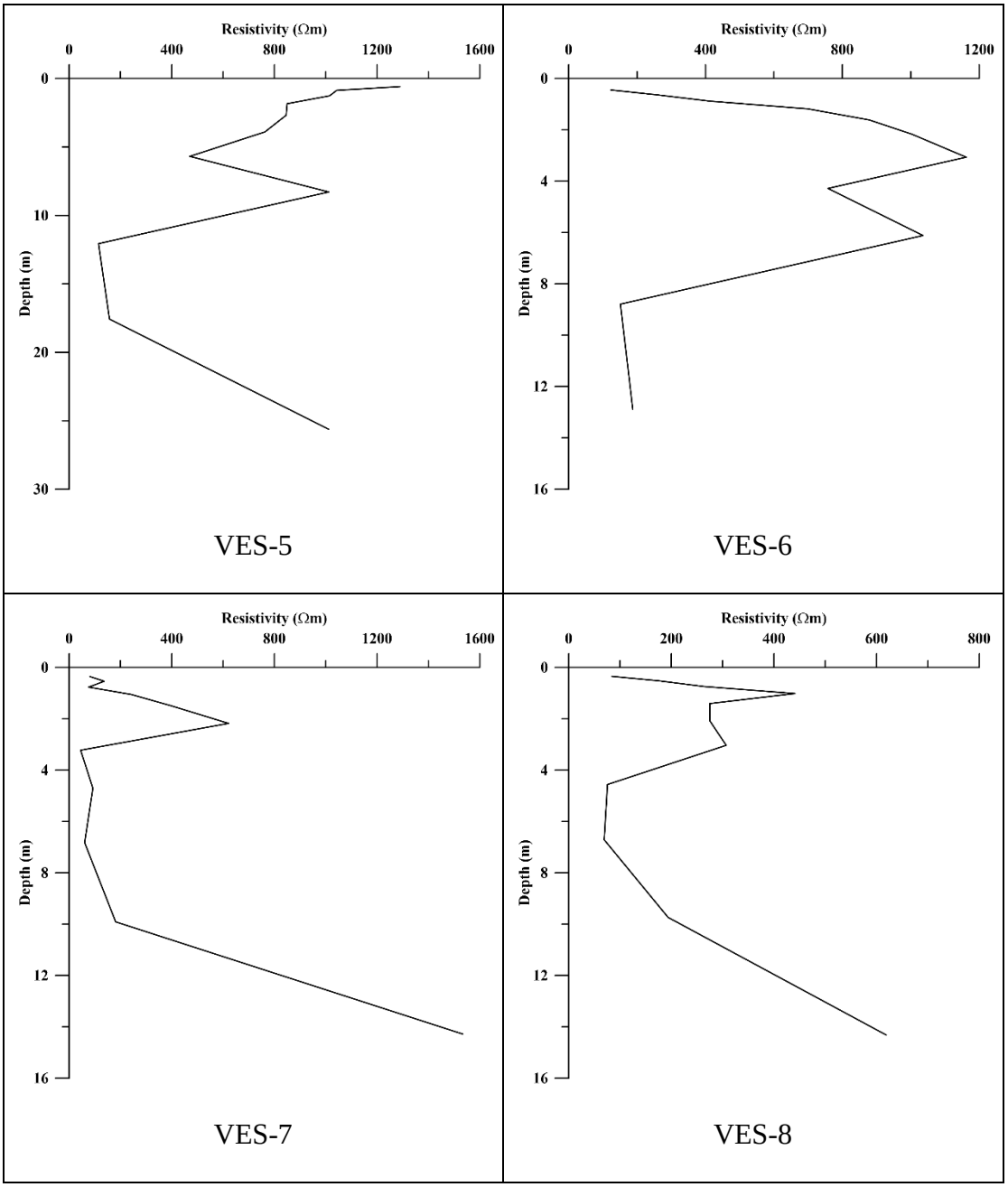
Resistivity (Ωm)
0
400
800
1200
1600
Depth (m)
0
10
20
30
VES-5
Resistivity (Ωm)
0
400
800
1200
Depth (m)
0
4
8
12
16
VES-6
Resistivity (Ωm)
0
400
800
1200
1600
Depth (m)
0
4
8
12
16
VES-7
Resistivity (Ωm)
0
200
400
600
800
Depth (m)
0
4
8
12
16
VES-8

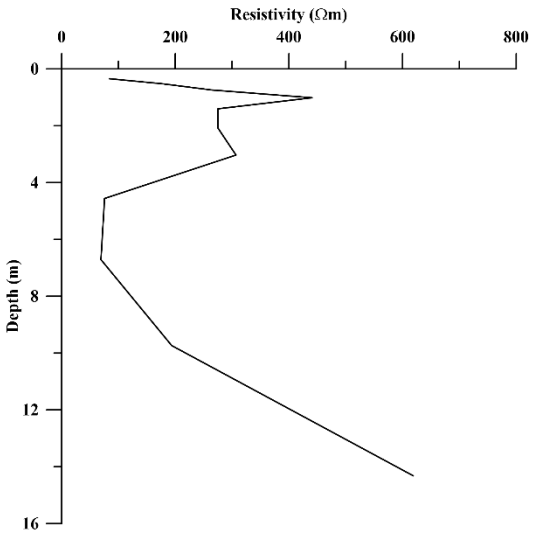

VES-9

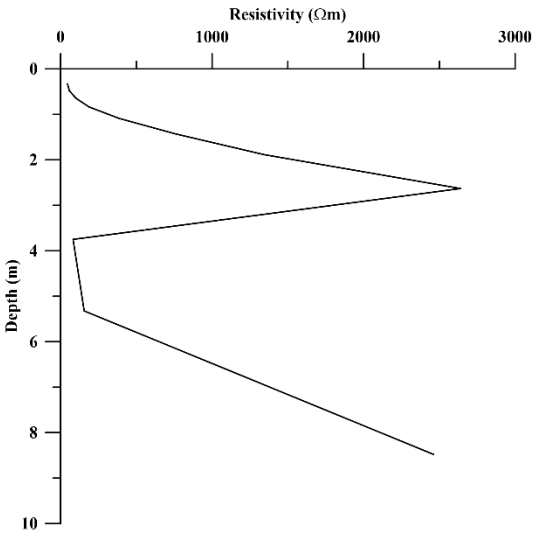

VES-10

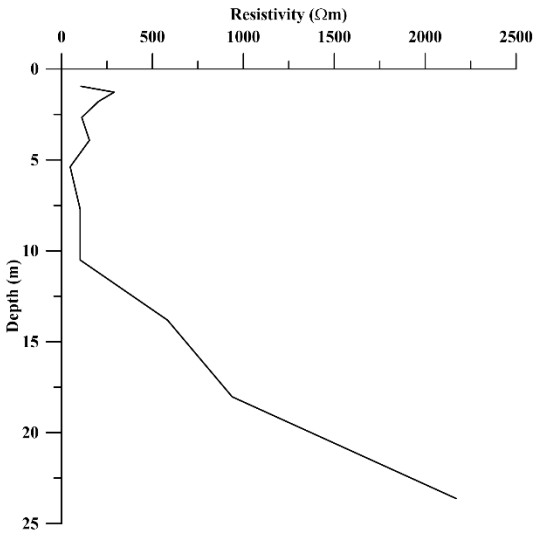

VES-11

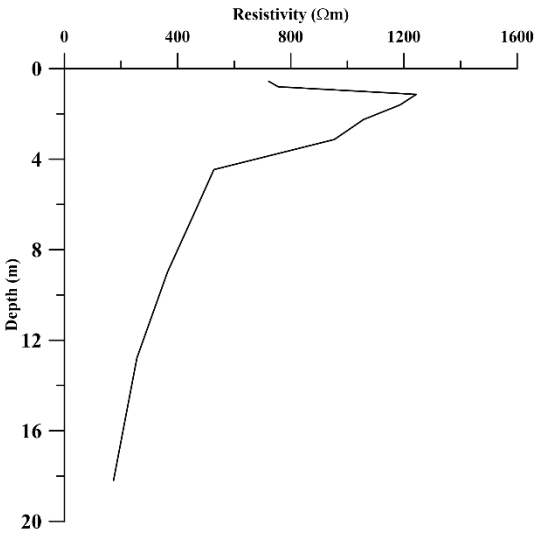

VES-12

APPENDICES III

Appendices III: Electrical resistivity tomography data for line one and line two.

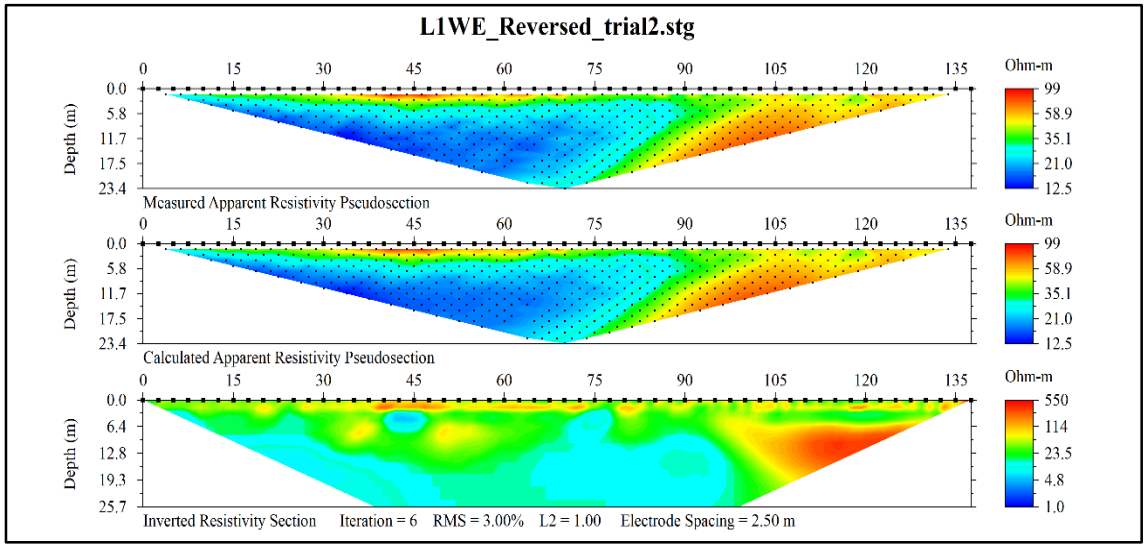

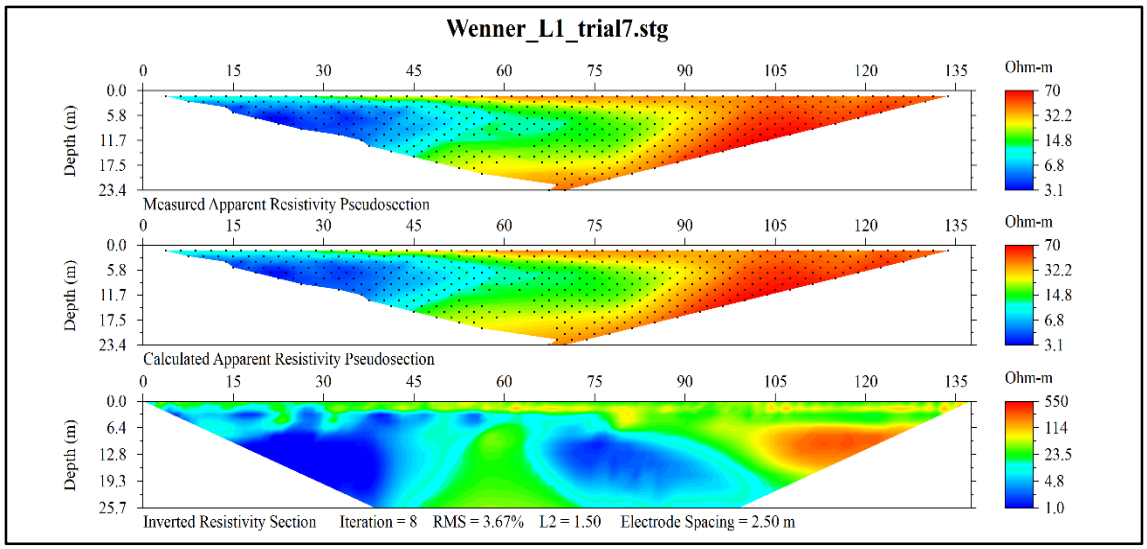

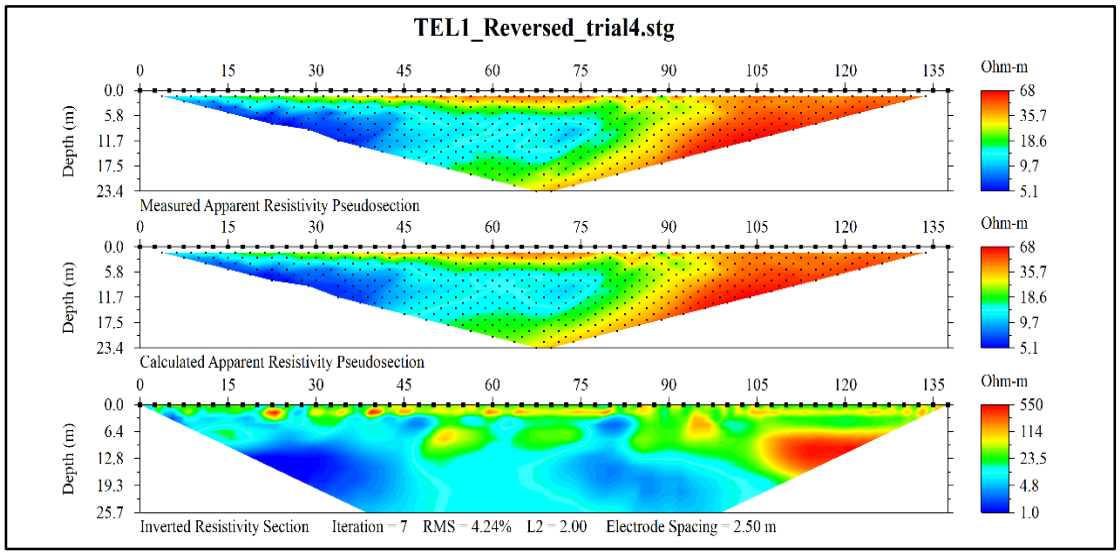

Line one March, June and September respectively.

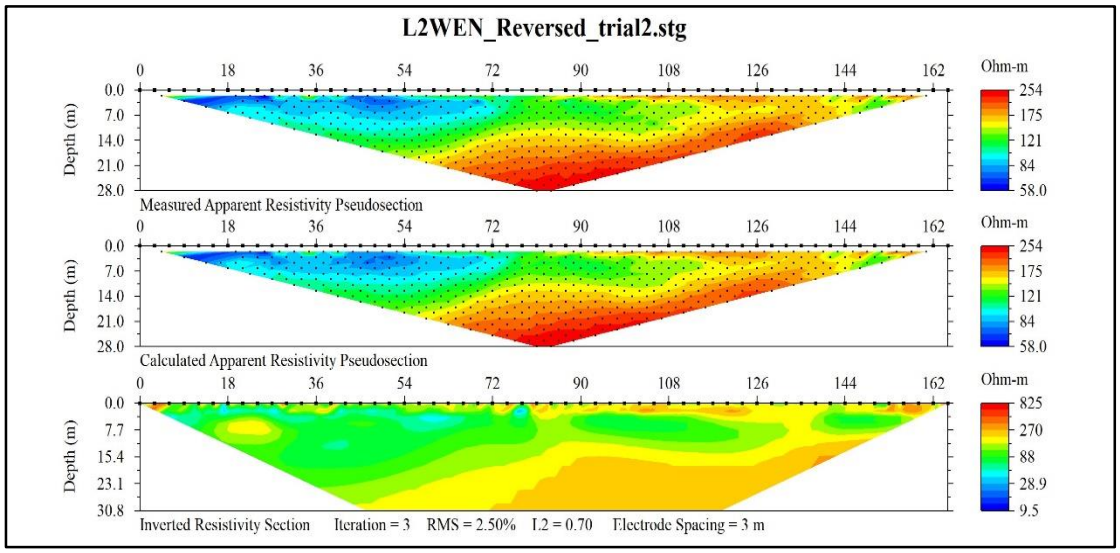

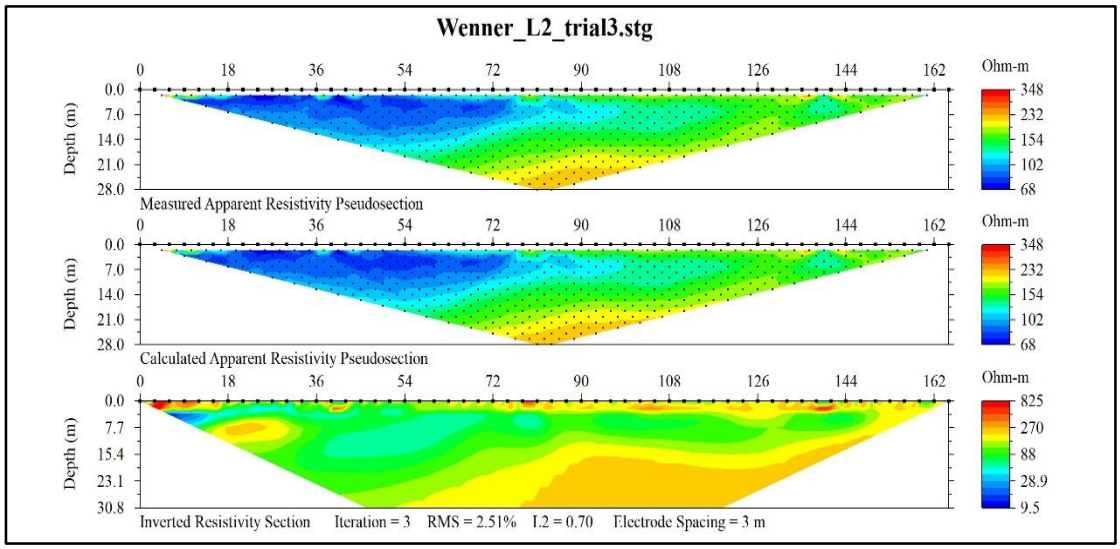

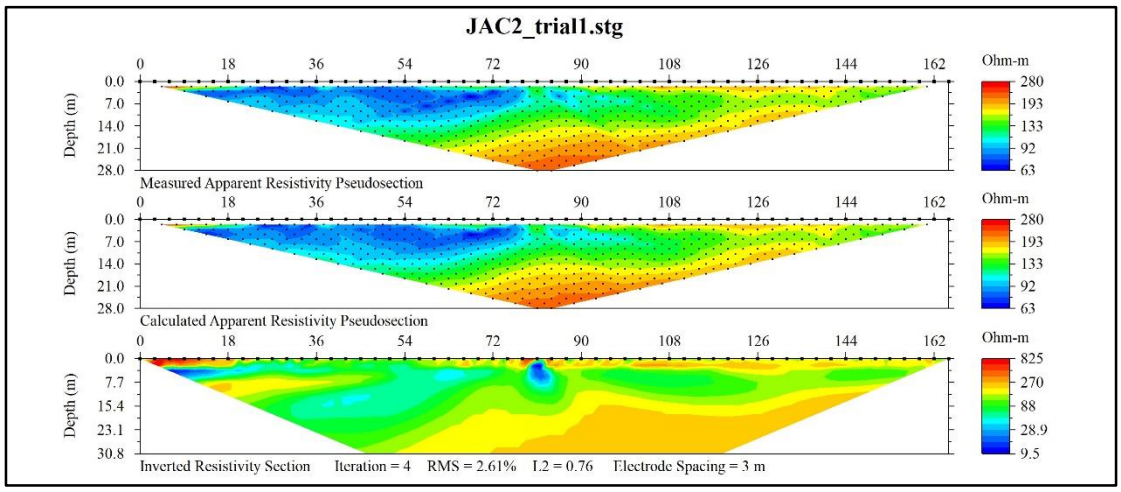

Line two March, June and September respectively.

VITAE

Name Yacob Tesfamariam Tesfaldet

Student ID 6030420011

Educational Attainment

Degree	Name of Institution	Year of Graduation
Master of Science (Earth System Science)	Prince of Songkla University Phuket Campus	2019

Scholarship and Awards during Enrolment

April 25, 2018:	Winning First Prize" in Research Poster Presentation Award 2018 in Prince of Songkla University (PSU), Phuket
Research Poster Title:	"*Vertical Electrical Sounding and Standard Penetration Test for Evaluation of Subsurface Soil in Phuket Island, Thailand*"
August 15, 2017	Thailand International Cooperation Agency Scholarship to pursue Master program at Prince of Songkla University (PSU)

Work – Position and Address

2015-2017	Graduate Assistant at Eritrea Institute of Technology (EIT)
2013-2015	Secondary School Teacher at Asmara Comprehensive Secondary School.

List of Publication

Yacob T. Tesfaldet and Avirut Puttiwongrak (2019). "Seasonal Groundwater Recharge Characterization using time-lapse Electrical Resistivity Tomography in the Thepkasattri Watershed on the Phuket Island, Thailand" *Hydrology, 6* (2), 36, 1-15.